University of Alberta

4-AMINOBENZOIC ACID HYDRAZIDE MEDIATED INHIBITION OF MICROPEROXIDASE-11: CATALYTIC INHIBITION BY REACTIVE METABOLITES

by

ARVADIA PRATIK

A thesis submitted to the Faculty of Graduate Studies and Research
in partial fulfillment of the requirements for the degree of

Master of Science
in
Pharmaceutical Sciences

Faculty of Pharmacy and Pharmaceutical Sciences

Fall 2011
Edmonton, Alberta

DEDICATION

This thesis is dedicated to my parents for their unconditional support

Abstract

Currently, there is lack of clinical therapeutics for inhibiting myeloperoxidase mediated pathogenesis. We used 4-aminobenzoic acid hydrazide (4-ABAH)[1], the most potent irreversible inhibitor of myeloperoxidase and microperoxidase-11 to obtain mechanistic insight on the role of reactive metabolites in catalytic inhibition. We investigated heme spectrum and peroxidase activity of MP-11 in the presence of 4-ABAH. Significant inhibition of MP-11 by 4-ABAH was observed. We performed ESR spin trapping studies on 4-ABAH reactive metabolites using 5,5-dimethyl-1-pyrroline-*N*-oxide (DMPO) and detected carbon-centered radicals. We performed MALDI and determined the change in elemental composition that occurred in these reactions. These masses were assigned to free radical metabolites of 4-ABAH and were not observed in reactions containing DMPO. We successfully determined MP-11 immunoreactivity using western blotting. We conclude that the 4-ABAH free radical metabolites bound to MP-11 were involved in the catalytic inhibition.

[1]Keywords – Peroxidase, Microperoxidase-11, 4-aminobenzoic acid hydrazide, ESR, DMPO, Myeloperoxidase, MALDI-TOF, Western blotting

ACKNOWLEDGEMENTS

I would like to express my first and foremost thanks to my supervisor Dr. Arno Siraki for providing me a wonderful opportunity to work in his laboratory.

This thesis could not have been completed without the help and support of my supervisor, *Dr.Siraki*.

I would also like to thank the members of my committee, *Dr.John Seubert* (Faculty of Pharmacy & Pharmaceutical Sciences, University of Alberta) and *Dr.Jason Acker* (Canadian Blood Services) for sharing your perspectives and broadening my experience.

I would like to acknowledge *Dr.Randy Whittal* (Department of Chemistry, University of Alberta), *Dr.Jack Uetrecht* (University of Toronto), *Dr.Ronald Mason* (NIEHS, NC, USA) and *Dr.Anna Chapman* (University of Otago) for their assistance on various aspects of this study.

I would like to thank Faculty of Pharmacy and Pharmaceutical Sciences and fellow graduate students.

Lastly, I would like to thank Canadian Institutes of Health Research (CIHR) for funding this work.

THESIS PUBLICATION

Arvadia P, Narwaley M, Whittal R, Siraki AG; 4-Aminobenzoic Acid Hydrazide Inhibition of Microperoxidase-11: Catalytic Inhibition by Reactive Metabolites. *Archives of Biochemistry and Biophysics* (Accepted)

Elsevier granted permission to include visible spectroscopy data, peroxidase activity data, Electron Spin Resonance spectra and Mass spectra in this thesis.

Contributions by authors

Arvadia Pratik performed the experimental work that includes designing, executing, collecting and interpreting spectra, enzyme activity assays. Assisted in the preparation of manuscripts

Malyaj Narwaley assisted in obtaining and preparing spectral data for publication.

Randy Whittal assisted in preparing and interpreting mass spectrometry data for the manuscript.

Arno G Siraki performed ESR experiments, interpreted the experimental data in all sectors, assisted in the writing and formatting this manuscript for publication.

Table of Contents

LIST OF TABLES

LIST OF FIGURES

LIST OF ABBREVATIONS

4-ABAH – 4-aminobenzoic acid hydrazide

BAH – Benzoic acid hydrazide/Benzhydrazide

DMPO – 5,5-dimethylpyrroline N-oxide

DTPA – Diethylenetriaminopentaacetic acid

EDTA – Ethylenediaminetetraacetic acid

EPR – Electron paramagnetic resonance

ESR – Electron spin resonance

FTICR – Fourier Transform Ion Cyclotron Resonance

H_2O_2 – Hydrogen peroxide

HCCA - α-Cyano-4-hydroxycinnamic acid

HOCl – Hypochlorous acid

HOSCN – Hypothiocyanous acid

HRP – Horseradish peroxidase

IC_{50} – Half maximal inhibitory concentration

IgG – Immunoglobulin G

INA – Isonicotinic Acid

INH – Isoniazid

KatG – Catalase-peroxidase

MALDI-TOF – Matrix Assisted Laser Desorption/Ionisation – Time Of Flight

MP-11 – Microperoxidase-11

MP-8 – Microperoxidase-8

MPO – Myeloperoxidase

MS – Mass Spectrometry

NAD – Nicotinamide Dinucleotide

NMR – Nuclear Magnetic Resonance

NOX – NADPH oxidase

O_2 - Oxygen

$O_2^{\cdot -}$ – Superoxide

POBN – α-(4-Pyridyl 1-oxide)-N-tert-butylnitrone

ROS – Reactive oxygen species

SDS-PAGE – Sodium Dodecyl Sulfate – Polyacrylamide Gel Electrophoresis

TBS – Tris-buffered saline

TFA – Trifluoroacetic acid

TRIS – Tris(hydroxymethyl)aminomethane

UV/Vis – Ultraviolet/Visible

λ_{max} – Wavelength of maximal absorbance

Chapter 1 - Introduction

1.1 Introduction

Myeloperoxidase is a vital enzyme for bacterial killing, present in human neutrophils[1]. It catalyzes the formation of hypochlorous acid (HOCl) a principal oxidant, from endogenous Cl^- and hydrogen peroxide. This acid is known to interact with many biomolecules and hence enzyme plays as an important role in inflammatory tissue injury[2]. Numerous compounds are known to inhibit myeloperoxidase[3]. These compounds can be used as future therapeutics for myeloperoxidase mediated inflammatory injury. Benzoic acid hydrazides are known to be irreversible inhibitor of myeloperoxidase activity[4]. They are known to inhibit HOCl production. The exact mechanism of inhibition is not defined. One of the proposed mechanisms is based on the generation of free radical intermediates of hydrazides[5]. The identity of free radicals involved in this inhibition is not characterized. In this study, we tried to investigate the mechanism of peroxidase inhibition by using microperoxidase-11 as a model system. We attempted to study the presence of free radical mechanism and also characterize the intermediate compounds involved in peroxidase inhibition.

1.2 Heme-peroxidases

Heme proteins are ubiquitous and indispensable for every living organism[6]. Peroxidases [EC 1.11.2] are the family of enzymes containing heme that have the ability to catalyze mainly one-electron oxidation of various substrates in the presence of hydrogen peroxide (H_2O_2)[7]. Some of the vital physiological functions associated with these metalloproteins includes oxidative catalysis, host-defense mechanism, electron & oxygen transport[8]. Peroxidases can

be found in species such as bacteria, fungi, plants and animals[7]. Based on sequential homology, peroxidases can be grouped into two superfamilies, i.e. peroxidase – cyclooxygenase (formerly - animal heme peroxidases) and peroxidase – catalase superfamily (combined heme-peroxidases of fungi, bacteria and plant origin)[9]. The animal heme peroxidase family is represented mainly through myeloperoxidase (MPO), lactoperoxidase (LPO), eosinophil peroxidase (EPO), thyroperoxidase, prostaglandin H synthase, peroxidasin, gastric peroxidases, uterine peroxidases and salivary peroxidases[10]. Structurally, peroxidases are composed of a polypeptide chain and its active site heme referred to as ferriprotoporphyrin IX[7]. Plant peroxidases such as horseradish peroxidase (HRP), yeast cytochrome c peroxidase (CcP) consist about 300 amino acids in their structure with non-covalently bound heme whereas the mammalian peroxidases are larger than in structure (576-738 amino acids) with covalently bound heme[11]. The oxidation state of iron in heme is Fe^{3+} in the case of native (resting) enzyme. The structure of heme present in the native peroxidase is composed of 4 pyrrole nitrogens bound to iron (Fe^{3+}) while the fifth coordination site is bound to a histidine residue via an imidazole side chain on the proximal side and the distal side is vacant[8]. In addition, the proximal histidine is bound to asparagine in mammalian peroxidases and with aspartic acid in the peroxidase-catalase superfamily. The catalytic cycle of xenobiotic oxidation by peroxidases is of similar nature to another hemeprotein, cytochrome P450 (CYP450) although there are wide differences in amino acid sequence homology[12]. A great deal of information on peroxidase based reactions is obtained from the peroxidase-

catalase family especially HRP used primarily to study enzyme kinetics. Hence, HRP has been used as model peroxidase enzyme to investigate the peroxidase reactivity towards xenobiotics[13]. The sequence of reactions involved in the xenobiotic transformation by peroxidases is described below.

$$\text{Peroxidases} + H_2O_2 \longrightarrow \text{Compound I} + H_2O \qquad [1]$$

$$\text{Compound I} + XOH \longrightarrow \text{Compound II} + XO^{\bullet} \qquad [2]$$

$$\text{Compound II} + XOH \longrightarrow \text{Peroxidase} + XO^{\bullet} + H_2O \qquad [3]$$

It can be observed from the above mentioned reactions that the enzyme is activated by hydrogen peroxide releasing a water molecule [eq.1]. Moreover, the formation of Compound I (Fe^{+4}) of the enzyme is observed [eq.1]. Compound I, a strong oxidant, oxidizes xenobiotic substrate (XOH) and itself gets converted to Compound II along with the formation of xenobiotic free radicals [eq.2]. Further, Compound II gets converted to resting peroxidase generating a free-radical and a water molecule [eq.3]. Thereby, substrates undergo one-electron oxidation steps twice. This cycle has being termed as redox cycling where the enzyme is regenerated to its original resting state at the end of the catalytic cycle[14]. The free-radicals generated during this cycle are of physiological significance since they can affect cellular functions[15]. For instance, oxidation of phenylhydrazine by animal peroxidases leads to the formation of phenyl radicals. Subsequently, enzyme gets covalently bound to these phenyl radicals and causes enzyme inactivation.

1.3 Myeloperoxidase (MPO)

Of all peroxidases, myeloperoxidase [EC 1.11.2.2] is biologically important for host defense and immunity[16]. MPO, a dimeric cationic protein, is present in azurophilic granules of neutrophils, monocytes, subcellularly in lysosomes and to minor amounts in macrophages[17]. It forms about 2-5% dry weight in human neutrophils. MPO expression is limited to myeloid cells. MPO is actively synthesized by granulocyte differentiation of promyelocytes and promyelomonocytes[18]. Structurally, MPO is composed of two sub-units linked to each other via disulphide (-S-S-) linkage. Individually, sub-units are termed as hemi-MPO that has molecular weight 73 kDa and 573 amino acids (Fig.1.3.1). Further hemi-MPO can be divided into heavy chain (58.5 kDa, 467 amino acids) and light chain (14.5 kDa, 106 amino acids)[17]. In mature MPO, the heavy chain contains heme and is glycosylated as an effect of post translational modifications. Unlike other peroxidases, myeloperoxidase has peculiar green colour that has characteristic ferric heme absorption of 428 nm called Soret Band (heme absorbance maxima)[19]. As a result, red shift is observed in the heme spectrum.

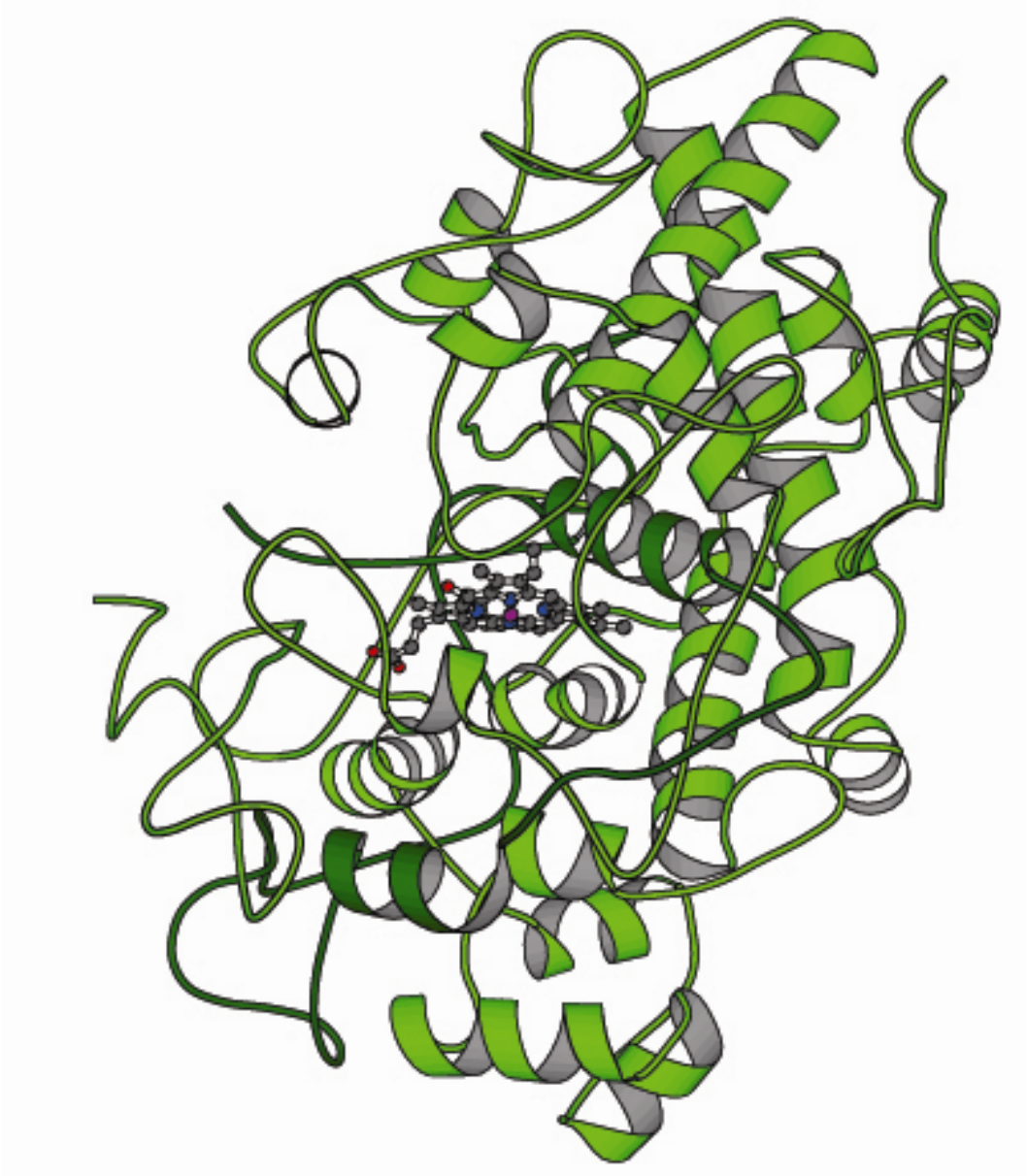

Fig.1.3.1 Ribbon representation of hemi-MPO with heme group in the centre[20].

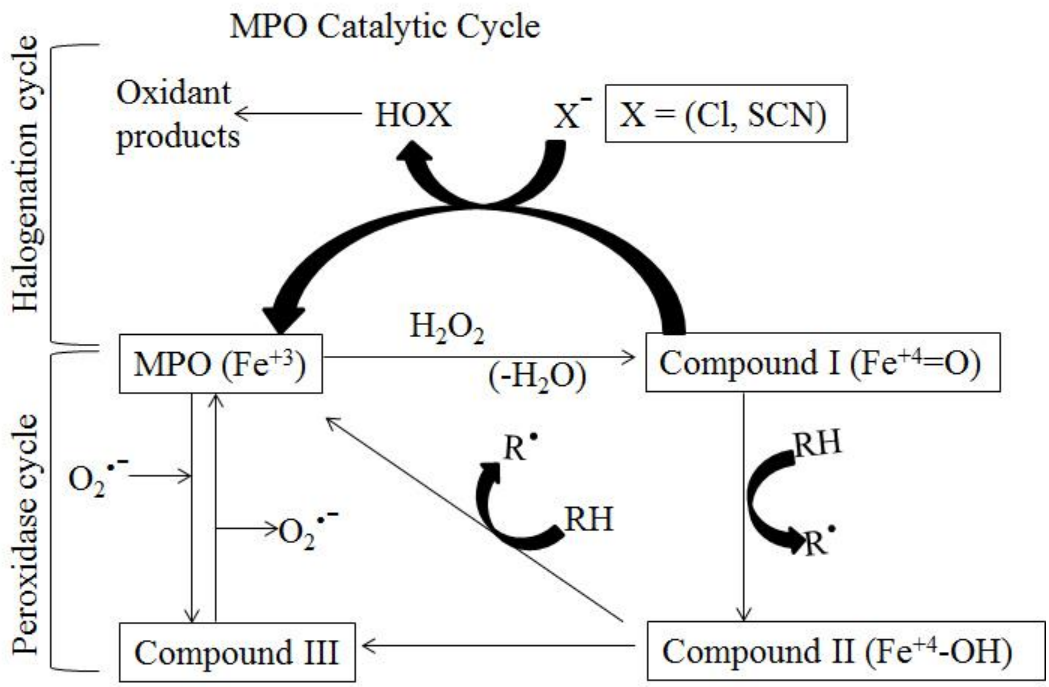

Fig.1.3.2 MPO catalytic cycle showing dual pathway of oxidation[17].

Resembling HRP, MPO catalyzes H_2O_2 based oxidation to form Compound I (Fig.1.3.2). In the presence of chloride, Compound I produces a strong oxidant hypochlorus acid (HOCl) and MPO is regenerated. However, in the absence of chloride, one-electron reduction pathways leading to Compound II and then to resting MPO takes place. Therefore, it can be said that MPO Compound I has the ability to oxidize a variety of substrates. Unlike HRP, excess H_2O_2 leads to the formation of Compound III, an inactive state of MPO which is slowly transformed back to resting MPO.

1.4 MPO mediated pathogenesis

Leukocytes are activated upon the recognition of pathogens. Activated leukocytes have bactericidal and viricidal properties since the potent oxidant HOCl produced by the action of MPO is responsible for bacterial killing[1]. Hence

MPO is considered to be an important enzyme for host defense. The *activation* of leukocytes, specifically neutrophils is an important step towards the bactericidal activity. Upon activation, neutrophils release MPO from the azurophilic granules into cytoplasm and thereby MPO is available for the $MPO/H_2O_2/Cl^-$ system[1]. This system has the ability to interact with the phagosome and later on assist in the process of phagocytosis. Therefore, it has been stated that MPO is required for optimal microbicidal activity in humans. In addition, HOCl or $MPO/H_2O_2/Cl^-$ has ability to oxidize various xenobiotics, particularly those containing nitrogen based functional groups. This metabolic biotransformation results in free-radicals of xenobiotics which may or may not be beneficial therapeutically. The significance of MPO in human body can be acclaimed in MPO deficient patients since they are exposed to higher risk of opportunistic reactions. It was reported in *in-vivo* experiments on MPO knock-out mice that *E.coli* were killed efficiently by activated leukocytes but *S.aureus* & fungi killing is dependent upon the presence of MPO[16]. It was reported that MPO-H_2O_2-halide system is toxic to several cellular systems such as bacteria, viruses, fungi, bacterial toxins, mammalian tumour cells, human granulocytes, lymphocytes, erythrocytes, chemical mediators – chemotactic factors, leukotrienes, matrix-metalloproteinase-7[17].

Contrastingly, the presence of MPO has been attributed as the basis of numerous pathophysiologies of diseases. The potent oxidants hypothiocyanous acid (HOSCN), hypobromous acid (HOBr) in addition to HOCl have been implicated as key intermediaries of tissues damage leading to inflammation and

myriad of other downstream signaling. As a result of these processes, MPO pathogenesis has been implicated in numerous diseases including atherosclerosis, cystic fibrosis, asthma, rheumatoid arthritis, nephritis, multiple sclerosis, Parkinson's disease and Alzheimer's disease[16]. Recently, myeloperoxidase activity was associated with urate formation and inflammation leading to gout[21].

1.5 MPO Inhibitors

The generation of peroxidase related oxidants plus the free-radicals including reactive oxygen species (ROS) should be controlled or scavenged in order to be able to prevent the tissue damage. Besides regulating the harmful catalytic effects of peroxidases, MPO inhibitors can be used to obtain mechanism related information on MPO activity. The production or removal of H_2O_2, required for the oxidation of halides by inhibiting NAPDH oxidase (NOX) is not a favorable approach to prevent biological damage[22]. It has been observed that inhibiting NOX and $O_2^{\bullet -}$ may also inhibit mitochondrial activity[23]. Hence chemical approaches for inhibiting MPO have been an attraction in this arena of research. Numerous compounds that inhibit MPO have been utilized to test their inhibitory efficiency[3,24]. Heme poisons such as carbon monoxide, cyanides and azides (bind to MPO heme) are not suitable as therapeutics due to toxicity profiles. They have high affinity for heme iron binding than oxygen and therefore cause permanent heme blockage. Plasma protein ceruloplasmin is a well-known MPO binding agent that inhibits peroxidase and halogenation activity of MPO[25]. However the nature of inhibition is reversible in the presence of anti-MPO antibodies. Also an alternate approach has been tested whereby compounds act as

a peroxidase substrate and diverts the peroxidase enzyme from its halogenation cycle. In this pathway, the weak oxidation of substrate by Compound I lead to formation of Compound II. Thus, the enzyme is trapped in the Compound II state and rendered catalytically inactive. As a result, generation of oxidants and hence tissue injury can be prevented. Compounds acting via such mechanism include some anti-inflammatory drugs[3,26], phenols, anilines, tryptophan and its derivatives[27], amino-acid tripeptides[70].

Certain limitations are implied in this inhibition strategy. These include 1) High concentration of substrate is required to overcome and outcompete halide oxidation; 2) Nature of inhibition is reversible since Compound II can be reduced to native enzyme by superoxide; 3) Specific to aromatic amines, it was been reported that MPO by virtue of peroxidation can metabolize these compounds to free-radicals that have other harmful biological effects such as agranulocytosis and systemic lupus erythematous[28,29]. Other compounds including hydroquinone[30] and acridine – amsacrine[31] have been reported inhibition for MPO mediated HOCl formation by Compound III formation. However it is assumed that the presence of $O_2^{\bullet -}$ will limit the inhibitory potential. The most promising MPO inhibitors are hydrazide and hydrazine compounds. There are considerable numbers of hydrazine/hydrazide compounds that can act as inhibitors[4]. They inactivate the enzyme and inhibit them irreversibly and hence they are known as "suicidal peroxidase substrates".

From the above information, it can be stated that MPO has been associated in pathogenesis of many diseases and also there are numerous compounds

available that regulate MPO activity. Despite these attempts, there are no clinically available peroxidase inhibitors. However, inhibiting MPO release from the granules can be looked as a potential therapeutic. Alternatively, MPO synthesis inhibitors must be explored as future therapeutics for MPO inhibition.

1.6 Hydrazides and its effects on peroxidases

Hydrazides are class of compounds containing (-$CONHNH_2$) functional group. It has been very long since the hydrazide classes of drugs were used as therapeutics in the market. Isoniazid (INH, pyridine-4-carboxy hydrazide) has been highly efficacious against *Mycobacterium tuberculosis* and has been used as a first-line agent in TB since 1952. Isoniazid, an aromatic hydrazide, is one of the most extensively studied drugs in various mammalian species for its metabolism. INH is activated and metabolized by catalase-peroxidase heme protein (KatG) system endogenously present in the mycobacterium species. Isoniazid acts as an irreversible MPO inhibitor[32]. Catalase-peroxidase dependent (KatGI) INH biotransformation results in the formation of isonicotinamide (INAAM) while (KatGII) will metabolize INH to isonicotinic acid (INA). In addition, free-radicals are also generated during the catalysis by KatG of the bacterium[33]. KatG catalyzed reaction leads to the formation of isonicotinoyl radicals from INH. Isonicotinoyl radicals with activated nicotinamide dinucleotide (NAD+) will form INH-NAD adduct to bind and inhibit the enzyme[34]. As a consequence, mycolic acid biosynthesis is inhibited and hence cell-death. Although INH is lethal to the mycobacterium, the mutation in KatG will lead to drug-resistance. It is reasoned that the acyl nucleophilic substitution pathway will be preferred over radical

formation and hence the effective spectrum of INH will be reduced. Human neutrophils containing MPO were reported to metabolize INH to INA in the presence of hypochlorus acid (Fig.1.6.1)[35].

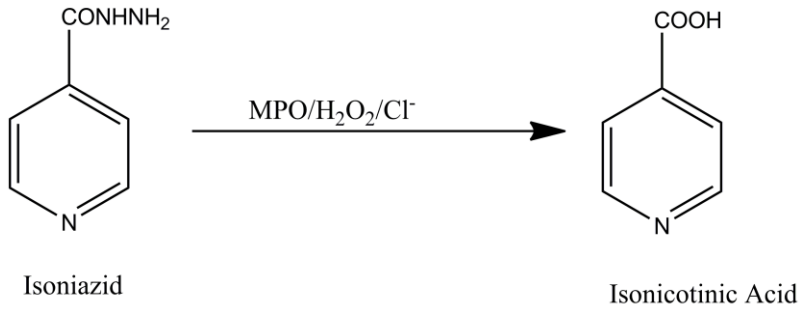

Fig.1.6.1 showing the MPO-halide system induced isoniazid conversion to isonicotinic acid

This metabolic conversion was additionally confirmed with the use of catalase. Catalase is the principle enzyme for breakdown of hydrogen peroxide into water and oxygen. Catalase prevented the oxidation of isoniazid in the activated leukocytes. It is worthwhile to consider the role of peroxidase mediated reactive metabolites in causing idiosyncratic drug reaction such as lupus and also hepatitis[12]. But there is no concrete evidence in support of this argument. The formation of isonicotinoyl radical from isoniazid is described but there is no indication of the other half of the molecule i.e. hydrazine moiety. Arylhydrazines like phenylhydrazine are metabolized by peroxidases into 8-hydroxymethyl derivatives[36]. Inhibition of horseradish peroxidases was confirmed by phenylhydrazine in presence of H_2O_2. The concept of "heme reactivity" with substrate and consequent modification was defined. Soret band/peak for most peroxidases is in the range 390nm – 450nm. It was stated that decrease in Soret band intensity of HRP with phenylhydrazine indicated the heme reactivity and

subsequent modification[37]. Besides, covalent adduct formation between enzyme and substrate leading to enzyme modification was proposed[5]. Hence, the structural elucidation was assessed using mass spectrometry and also with ^{1}H NMR (Nuclear Magnetic Resonance)[38]. This study had opened an important aspect on substrate reactivity with heme peroxidases. It provided valuable insights into catalytic mechanism of peroxidases and this research can be extrapolated in predicting the reactivity of various heme substrates.

Another important class of hydrazide compound that has been extensively studied is benzoic acid hydrazides. Benzoic acid hydrazide (BAH) (Fig. 1.6.2) and its derivatives have been described as metabolically activated irreversible MPO inhibitors[4]. Formation of free radical metabolites of hydrazides with peroxidases has been well established in the past using primarily HRP as the model enzyme[5]. Apparently, BAH mediated HRP modification was viewed by employing benzoyl-heme adduct isolation and measurement by mass spectrometry. The site of BAH metabolite linkage to HRP heme was assumed at δ-meso-position of protoporphyrin IX. The mechanism behind such reactivity was proposed via formation of free-radical intermediates. Further, BAH free radicals mediated the conversion of MPO to Compound III. 4-Aminobenzoic acid hydrazide (4-ABAH) (Fig. 1.6.2) is the most potent inhibitor of HOCl production. 4-ABAH is a mechanism based irreversible MPO inhibitor that inactivates MPO in the presence of H_2O_2. Also, it was reported that 4-ABAH can undergo metal-catalyzed autoxidation by MPO without the requirement of H_2O_2[39]. It is likely that the 4-ABAH oxidation by peroxidases follows the mechanism below in trace

metal free solution. As shown in eq.4, resting state MPO gets converted to Compound I by H_2O_2 catalysis. Compound I will further catalyze hydrazide substrate to free radical derivative of hydrazide [eq.5]. This would then be further metabolized by Compound II to generate carbonyl and hydrazyl radicals [eq.6].

MPO^{3+}(resting state) + H_2O_2 $\longrightarrow$ Compound I + H_2O **[4]**

$R\text{-}CO\text{-}NH\text{-}NH_2$ + Compound I $\longrightarrow$ $CO\text{-}NH\text{-}NH^{\bullet}$ + Compound II + H^+ **[5]**

(Primary radical species)

Compound II + $R\text{-}CO\text{-}NH\text{-}NH^{\bullet}$ $\longrightarrow$ $R\text{-}CO^{\bullet}$ + $NH{=}HN^{\bullet}$ + MPO^{3+} **[6]**

(where R = 4-aminobenzene)

Moreover, this inhibition is associated with irreversible damage to heme prosthetic group as inferred from the spectral changes[40]. The propensity of free radical formation and subsequent enzyme inhibition increases with high concentrations of hydrogen peroxide and low availability of oxygen. Unlike MPO, HRP does not achieve Compound III state and therefore most of the mechanism based on HRP does not reflect the complete reactivity of the substrates that can be extrapolated to MPO.

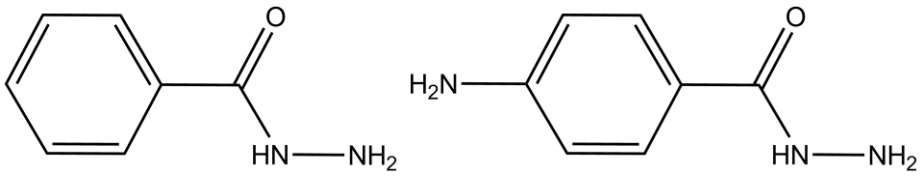

Fig.1.6.2 Chemical Structure of BAH & 4-ABAH

1.7 Microperoxidases

Microperoxidases are the ferric-heme containing family of peroxidases that are isolated from cytochrome C by enzymatic digestion[41]. Human cytochrome C is a heme protein that has molecular weight of 12.38 kDa[42]. Cytochrome c is found in the inner membrane of the mitochondrion and is a component of electron transport chain. Microperoxidases are named accordingly depending upon the number of amino acid residues in the polypeptide chain. Microperoxidase-11 (MP-11) is a 1.8 kDa undecapeptide isolated from mammalian cytochrome C. It contains amino acid residues 11-21 with the heme moiety covalently linked to the polypeptide chain (Fig.1.7). Like peroxidases, MP-11 has the fifth co-ordination position of iron occupied by the histidine while the distal site is exposed and available for substrate reactivity.

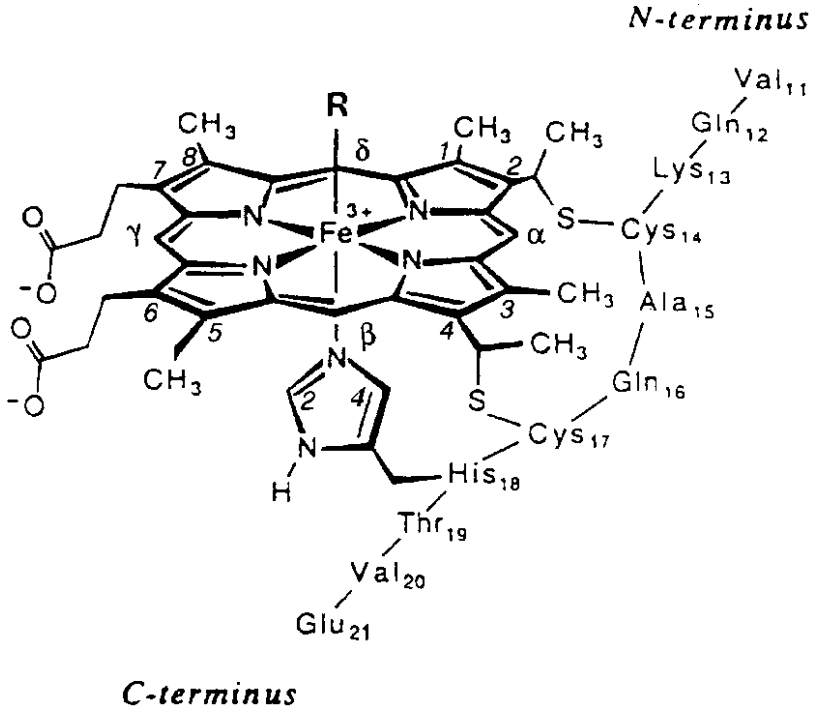

Fig.1.7 Microperoxidase-11 showing the amino acid sequence and linkage with heme ring via sulphide linkage through cysteine[43].

Even though the catalytic turnover is less, microperoxidases have the ability to mimic peroxidation reactions in the presence of H_2O_2. Besides being pseudo peroxidase, it can undergo the peroxidase cycle with typical compound state formation that has yet to be fully characterized. MP-8 is known to catalyze oxidation reactions of aromatic hydrocarbons specifically aniline compounds[44]. Heme bleaching and peroxidase activity can be perceived in similar fashion in MP-11 with the excessive use of H_2O_2, as evident in HRP[45]. Therefore, the use of MP-11 as a kinetic model for peroxidases was validated. MP-11 is said to be a peroxidase with extensive specificity for hydrogen peroxide, *tert*-butyl hydroperoxide, superoxide and hydroxyl radicals[46]. It was also reported that MP-11 is an anti-cataract agent[47]. It acts by reacting and eliminating H_2O_2 with the help of free radical scavenging agents such as ascorbic acid. Considering its peroxidase behaviour and uncomplicated structure, we employed MP-11 as a model peroxidase system to investigate protein modification induced by 4-ABAH. Since myeloperoxidase is a complex protein structure, limited analytical techniques are applicable and MP-11 can be used instead. A fairly new area of research may be established to define a model for understanding the molecular mechanism of 4-ABAH and other hydrazides.

1.8 Immuno-spin trapping

Electron spin resonance (ESR) or electron paramagnetic resonance (EPR) is widely used technique to detect the presence and characterize free radicals species. ESR spectra can provide vital structural information. But the stability of free radicals has always been an issue in the past and the present. ESR with stopped flow technique was used for rapid determination of the primary radical species[48]. Earlier approaches in free radical chemistry were to detect them as soon as they were formed since the free radicals species are short-lived (Fig.1.8.1). Therefore, spin trapping has been applied for trapping the free radicals using primarily nitrones and nitroso spin traps[49]. Signals detected from stable spin adducts are long lived as compared to direct ESR (Fig.1.8.1). Nitrone spin traps include 5,5-dimethylpyrroline N-oxide (DMPO), α-(4-Pyridyl 1-oxide)-N-tert-butylnitrone which forms nitroxide adducts with C, O and S-centered free radicals. While major nitroso spin traps are 2-methyl-2-nitrosopropane (MNP), 3,5-dibromo-4-nitrosobenzene sulfonate (DBNBS) can add free radicals to the nitrogen of nitroso group[50]. One of the crucial parameter in determining the identity of the free radicals is "hyperfine splitting constant" of the spectrum[51]. Protein derived radicals can be detected directly using ESR and/or with spin trapping ESR. Thus, ESR can be employed to obtain the detailed insight into the mechanism of protein/amino acid free radical formation. Besides, ESR has been used for *in vivo* detection of free radical metabolites of xenobiotics[52]. The potential limitation of using ESR in case of proteins is the requirement of significant amount of proteins. Heme peroxidases have been subject of interest

since protein free radicals formation has been detected by ESR[50]. With respect to hydrazides, carbon centered radicals were detected in ESR with isoniazid/HRP/H_2O_2 system using DMPO as spin trap at pH 10 and under nitrogen gas. The free radical formation proceeded via the unstable primary radical (R-CONHNH$^{\cdot}$) that dissociated into C-centered radical (R-CO$^{\cdot}$) and di-imide (NH=NH). The former radical species was detected in ESR spectrum as DMPO-nitrone adduct at with splitting constants (a^N = 15.6G and a^H = 18.8G)[39]. Another study had confirmed the same radical species using spin trap 2,2,6,6,-tetramethylpiperidine-1-oxyl (TEMPO)[53]. DMPO has been widely used in living systems due to its stability in redox environment and low toxicity.

Development of antibody against DMPO-nitrone adduct has significantly improved the specificity and sensitivity for free radical detection in biological systems[50]. When protein or amino acid radical is formed in the system, it is trapped by DMPO via covalent linkage (Fig. 1.8.2). This DMPO-nitrone adduct is fairly stable for long time and hence immunological detection is achievable. In addition, the capacity of anti-DMPO serum for recognizing DNA radicals has been confirmed[54]. Hence, these methodologies can be used to characterize the 4-ABAH free radical intermediates responsible for myeloperoxidase inhibition. Concomitant protein residue modification can be studied using DMPO through western blotting and ELISA (enzyme linked immunosorbant assay).

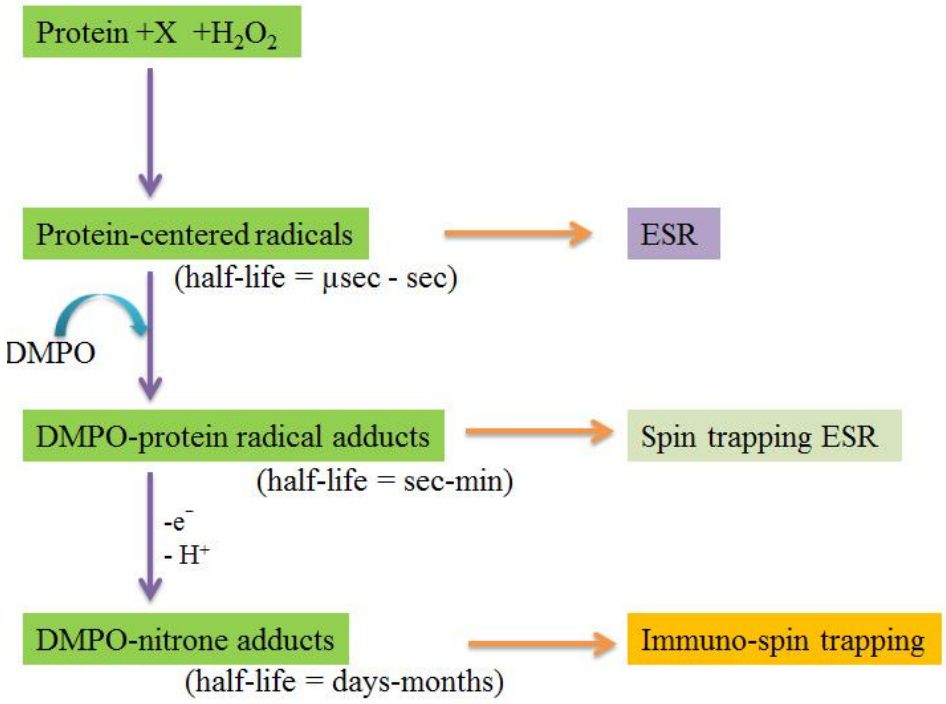

Fig.1.8.1 Schematic representation of protein-radical detection by spin trapping[50]

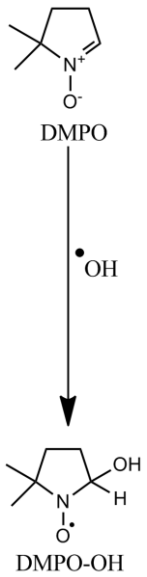

Fig.1.8.2 represents the DMPO mechanism of free radical trapping by covalent linkage[50]

1.9 Hypothesis

It is well known that MPO is irreversibly inhibited by 4-ABAH. We hypothesize that 4-ABAH will inhibit MP-11 via a free radical mechanism (Fig 1.9). The free radicals will form covalent adducts with MP-11. The same free radicals could be generated and detected with MPO which are responsible for MPO inhibition.

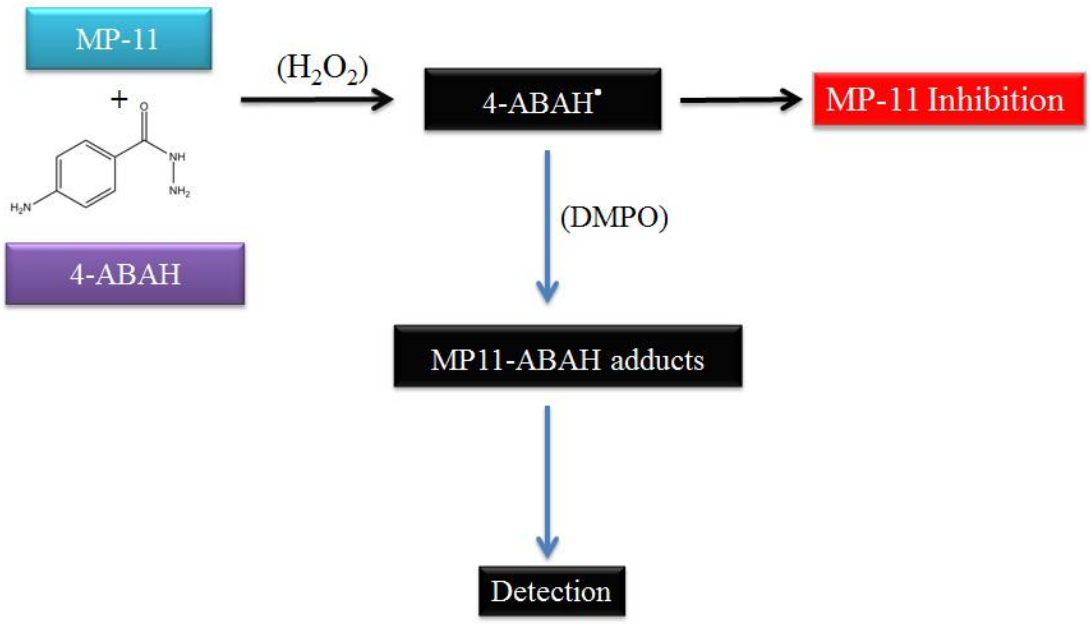

Fig.1.9 Schematic representation of the hypothesis on MP-11 inhibition by 4-ABAH

Chapter 2 - Materials and Methods

2.1 Chemicals

MP-11 (equine heart cytochrome c), 4-ABAH, diethylenetriaminopentaacetic acid (DTPA), sodium phosphate monobasic and dibasic, hydrogen peroxide (50%), guaiacol, tris(hydroxymethyl)aminomethane (TRIS), sodium chloride, potassium chloride, glycine, sodium dodecyl sulfate (SDS), cold water fish skin gelatin were obtained from Sigma-Aldrich Co. (Oakville, ON, Canada). HPLC grade water was purchased from Caledon Laboratory Ltd. (Georgetown, ON). Chelex-100 resin, nitrocellulose membrane, extra-thick filter pads were purchased from Bio-Rad Laboratories (Mississauga, ON). HCCA (α-Cyano-4-hydroxycinnamic acid), acetone and acetonitrile were kindly provided by Mass Spectrometry Facility, Department of Chemistry at University of Alberta. Anti-DMPO antibodies were obtained from Cederlane (Burlington, ON)

2.2 Reaction Conditions

HPLC grade water was used to prepare all the aqueous solutions unless otherwise stated. All the chemicals were of highest purity available. MP-11 solution was prepared in water and its concentration was determined at 399 nm with extinction co-efficient of 0.176 $m^2 \cdot mol^{-1}$ [55]. 4-Aminobenzoic acid was dissolved in water at 60˚C. The concentration of hydrogen peroxide (30% v/v) was estimated by its molar extinction co-efficient (43.6 $m^2 \cdot mol^{-1}$ at 240 nm) and a stock solution was prepared by dilution in water[56]. All the solutions were stored at 4˚C unless when used.

2.3 Spectrophotometry

2.3.1 Peroxidase Activity Assay

Kinetic scans were recorded every minute for 20 minutes to measure the peroxidase activity by guaiacol assay (Fig. 2.3.1)[57]. Scans were performed in a clear 96 well plate using kinetic mode in Multiskan EX Microplate Photometer (Thermo Scientific, Canada). The concentrations of the reactants were the same as above except DMPO (100 mM). The reactions were incubated in 1.5 mL microtubes at 35˚C for 30 minutes. These solutions were then diluted 10-fold and the peroxidase activity was measured by the addition of 0.6 mM guaiacol and 0.6 mM H_2O_2 in each given reaction[58]. The experiment was performed in a 96-well plate and the reactions were monitored each minute at 450 nm at room temperature (Fig.2.3.1). The data obtained from these experiments were used for further calculations. The experiment was repeated for a maximum of 3 times. IC_{50} value of 4-ABAH for MP-11 was determined via concentration-dependent MP-11 peroxidation inhibition using guaiacol assay described above. The concentration of 4-ABAH used in the experiment had a range from 0.05 mM to 5 mM while the MP-11 was incubated alone without any substrate as a negative control. The same reaction conditions were followed as mentioned for determining the peroxidation inhibition. The data for this experiment was obtained by repeating the experiment for a maximum of 3 times. The IC_{50} value was calculated by hyperbolic curve fitting method using Sigma Plot (Systat Software Inc., Chicago, IL, USA).

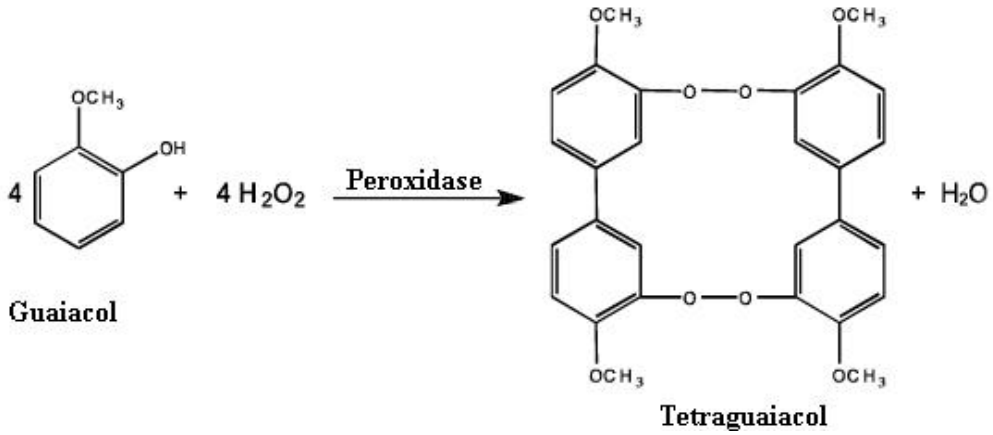

Fig.2.3.1 Reaction of guaiacol in peroxidase activity assay to form tetraguaiacol.

2.3.2 Heme spectra

Spectrophotometric scans were performed with Beckman Coulter DU-730 Life Science UV/Vis spectrophotometer using a quartz cuvette. HPLC grade water was used in preparing the reaction mixtures. The spectrophotometer was set to wavelength scan mode and the reading was water-blanked. The concentration of reactants used in the experiment were MP-11 (1 µM), DMPO (10 mM), H_2O_2 (50 µM), 4-ABAH (200 µM). MP-11 was added to cuvette in 500 µL total volume, mixed and was scanned between 350 nm to 450 nm at ambient temperature conditions. Further, H_2O_2, 4-ABAH and DMPO were added and subsequently scanned. Addition of each reactant was measured individually. The addition of reactant in any given set of reactions was initiated with MP-11 alone in each case, followed by H_2O_2 and finally with 4-ABAH. Spectra were recorded 5 minutes and 30 minutes after the addition of final reagents. The cuvette was thoroughly washed after each reaction to limit traces of previous reaction mixtures. The observations were recorded into the instrumental memory and

further graphical data was generated from raw data by importing data from .csv (comma separated value) file in Microsoft Excel Spreadsheet.

2.4 Electron Spin Resonance Measurements

ESR spectra were obtained using Bruker Elexsys E500 series spectrometer at Department of Biochemistry, University of Alberta. Instrument parameters were set to the following: frequency = 9.79 GHz, modulation = 100 kHz, modulation amplitude = 0.4 G, power = 20 mW, gain = 60 dB, scan time = 163 s, time constant = 163 ms. The instrumental parameters were set to conditions specific for detection of DMPO-nitrone based free radical adducts. Samples were prepared in a 0.1 M phosphate buffer at pH 7.3 (Chelex-treated with 100 µM DTPA). MP-11 (100 µM), DMPO (100 mM) H_2O_2 (1.5 mM), 4-ABAH (3 mM) and BAH (3 mM) were used in various reactions with total volume of 200 µL per reaction. These reactions were initiated by addition of MP-11. The samples were vortexed and transferred from microtubes to a quartz flat cell and the resulting spectrum was recorded. The flat cell was washed and cleaned completely before and after each reaction with distilled water and/or ethanol to ensure the complete removal of the previous reaction mixtures. The raw data from the spectrum were recorded in .csv file format. It was then imported to Microsoft Excel spreadsheet for preparation of graphical data.

2.5 Mass Spectrometry

Low-resolution MALDI (Matrix Assisted Laser Desorption Ionization Mass Spectrometry) analysis was performed using a Voyager Elite (AB Sciex, Foster City, CA, U.S.A.) time-of-flight mass spectrometer. The instrument was

operated at 20 kV in positive ion delayed-extraction mode using the reflectron setting and pulsed nitrogen laser (337 nm). (4). HCCA (α-Cyano-4-hydroxycinnamic acid) was used as the matrix for the analysis. HCCA matrix was prepared as 1 – 2 $kg \cdot m^{-3}$ in methanol: water (9:1). Samples were prepared in HPLC grade water. All reactions were incubated at 35˚C for 30 minutes prior to MALDI analysis. Two layer sample preparation method as well as dried-droplet method was employed for sample plate preparation[59]. Initially, the first layer of HCCA (1 µL) was spotted and allowed to dry onto the MALDI sample plate (AB Biosystems). While various reaction mixtures were mixed with 0.1% TFA (trifluoroacetic acid) and HCCA matrix in (1:1:2) proportions. TFA was purposely used to acidify the samples. The above mentioned sample (0.5-0.8 µL) was then carefully layered on top of the first layer (HCCA). The plate was injected into the instrument and measurements were carried out under room temperature conditions. This analytical method was validated for the experimental purpose by repeated measurements of MP-11 (100 µM).

High-resolution MALDI analysis was completed on a Bruker Daltonics (Billerica, MA, USA) 9.4T Apex Qe FTICR (Fourier transform ion cyclotron resonance) mass spectrometer equipped with an Apollo II Dual ion source which includes a pulsed nitrogen laser. The instrument was calibrated externally using sodium cationized polyethylene glycol with trans-2-[3-(4-tert-Butylphenyl)-2-methyl-2-propenylidene] malononitrile as matrix prior to acquisition of the samples on a stainless steel sample target. Samples were analyzed using HCCA as matrix with 1 mM $NH_4H_2PO_4$ added and spotted on an AnchorChip target

(Bruker Daltonics). Molecular formula analysis was performed using Generate Molecular Formula (GMF) tool in DataAnalysis (Bruker Daltonics).

2.6 Western Blotting

Western blots were performed using 10% polyacrylamide gel consisting of 10% glycerol due to the low molecular weight of MP-11[60]. The presence of glycerol in the gel reduces the protein mobility and therefore leads to good resolution of small molecules. The samples containing various reactants were mixed with 5x non-reducing pink tracking dye (Thermo Scientific, Canada). Samples were incubated at 35˚C for 30 minutes and then were run under non-reducing conditions. The gels were loaded with 30 µL samples in each well. The concentration of proteins loaded in each well was 5 µg based on the calculation from the stock solution concentration. Samples were run using the Mini-Protean® system (Bio-Rad Laboratories, Mississauga, ON). Initially, the instrument was operated at 120 V for 10-15 minutes after which the voltage was increased to 150 V for faster sample run. After sufficient resolution, the gel was removed from the instrument and incubated in transfer buffer for 5-10 minutes. The proteins were transferred from the gel to nitrocellulose membrane using a Trans-Blot SD Semi-Dry Transfer Cell (Bio-Rad Laboratories). Since the gel was thick and low molecular weight protein was involved, transfer time was optimized using various voltage settings within the instrument. The optimum transfer condition for this custom gel in semi-dry assembly is 15 V for 15 minutes. Membranes were blocked with 4% cold fish gelatin in pH 7.4 Tris-buffered saline (TBS) containing 0.05% Tween-20 for 1 hour at ambient temperature. After a 5 minute wash, the

primary antibody (rabbit anti-DMPO polyclonal) (1:50,000) in washing buffer was incubated for 1 hour at room temperature. Membranes were then washed with washing buffer for 30 minutes. Further they were incubated with a goat anti-rabbit conjugated to horseradish peroxidase (HRP) secondary antibody (goat anti-rabbit) (1:100,000) for 1 hour at room temperature. Washing step was repeated for 30 minutes and then membrane were treated with 500 µL of luminol based enhanced chemiluminiscence substrate (ECL Advance, GE Healthcare) for 30-50 seconds. Protein expression was detected by means of chemiluminiscence on an x-ray film (CL-Xposure 5"x7" X-ray film, Thermo Scientific, Canada). In another experiment, the primary antibody was changed to "mouse anti-DMPO monoclonal" in strength 1:100,000 and secondary antibody "rabbit anti-mouse HRPO" at 1:200,000 strength. Also, experiments were performed using a custom antibody (anti-isonicotinoyl), synthesized for detecting isonicotinoyl metabolites. The primary anti-isonicotinoyl antibody (1:50,000) and secondary goat anti-rabbit HRPO (1:100,000) was used. The detection process was performed as described previously. Further, the reactants were assessed in an alkaline phosphatase based chemiluminiscence detection system. The reaction conditions were same as described previously. Antibody concentrations were optimized for this detection system. As a result, the primary antibody rabbit anti-DMPO (1:5000) and secondary antibody goat anti-rabbit alkaline phosphatase (1:10,000) was used. The membrane was finally treated with 500 uL of alkaline phosphate substrate (CDP-star, EMD Biosciences Inc.) for 30-50 seconds and developed on an x-ray film. In one of the experiments, the gel containing the various reactions was

transferred into nitrocellulose membrane following the same procedure as above and was subjected to chemiluminscence substrate for developing the film. Also, the membrane was blocked with 4% gelatin in TBS in one instance and then exposed to chemiluminscence substrate. Finally in a separate experiment, the membrane was blocked as above and only secondary HRPO antibody was incubated at room temperature for 60 minutes. This membrane was further developed using chemiluminiscence substrate as above. In each of the above mentioned experiments, control reactions included either MP-11 alone or MP-11 + H_2O_2.

2.7 Statistical Analysis

Sigma plot 10.0 was used to perform statistical analysis of the experimental data. All the results in the peroxidase activity are presented as the mean ± standard error. Pairwise multiple *post-hoc* comparison procedure (Student Newman Keuls Method) was used for comparison with significance ($p<0.001$). IC_{50} value for 4-ABAH was calculated from Four Parameter Logistic equation using hyperbolic curve fitting method.

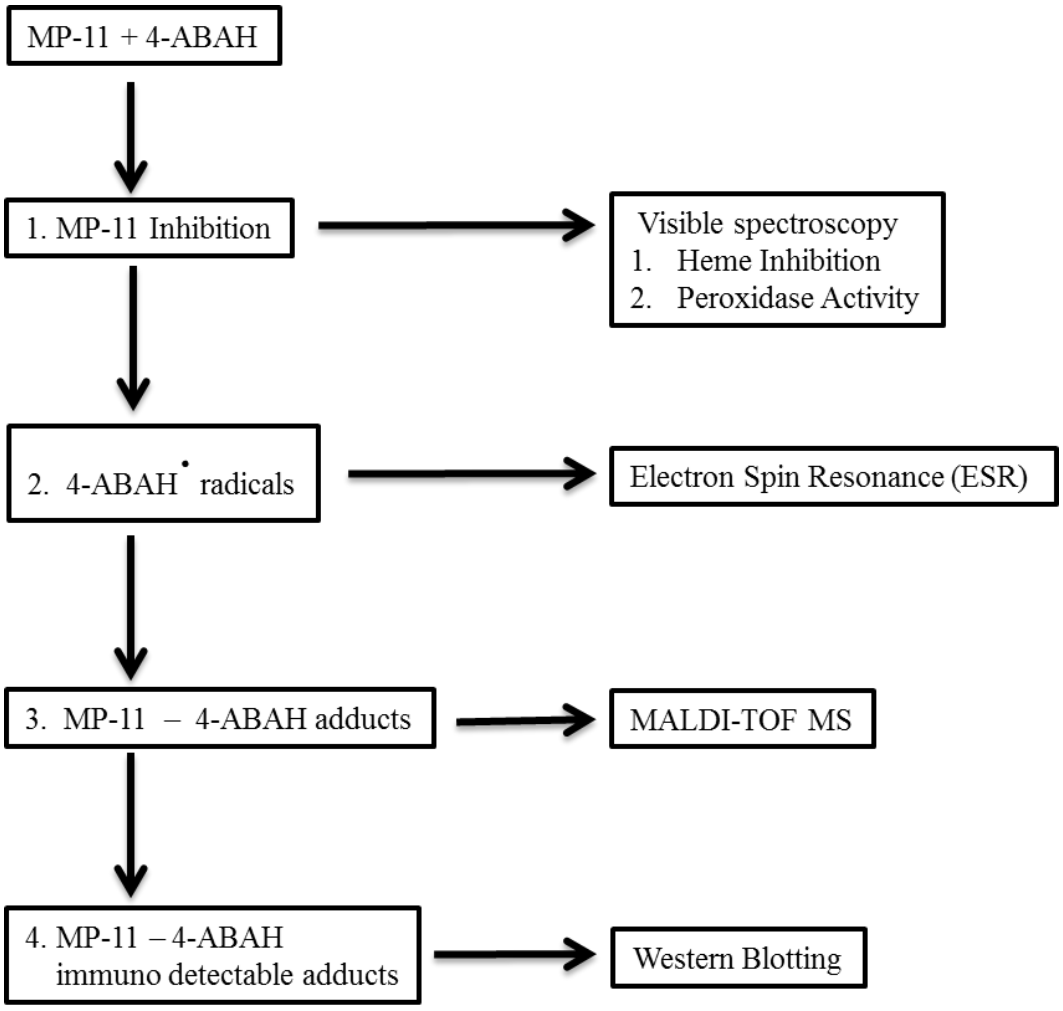

Fig. 2.7 Schematic representation of Workflow analysis.

Chapter 3 - Results

3.1 Peroxidase activity of MP-11 incubations

MP-11 peroxidase activity was assessed spectrophotometrically by monitoring the oxidation of product of guaiacol (tetraguaiacol) at 450 nm[41]. We used varying concentrations of 4-ABAH with 1 μM MP-11 and derived the IC_{50} (179.1 ± 32.8 μM) from an inhibition curve (Fig. 3.1). In addition, we wished to determine if DMPO could have an effect on preventing 4-ABAH mediated inhibition of MP-11. This was carried out since free radical metabolites of 4-ABAH were proposed to be involved in the mechanism of inhibition for other peroxidases[40]. In Table 1, we show the absorption of guaiacol after 10 minute incubation for peroxidase activity with different treatments of MP-11. 4-ABAH inhibited guaiacol oxidation significantly ($p<0.001$); but in the presence of DMPO there was significantly more oxidation of guaiacol suggesting that MP-11 inhibition by 4-ABAH was attenuated. To determine if greater inhibition would occur with H_2O_2 to catalyze 4-ABAH oxidation, we assayed peroxidase activity after incubation of MP-11 with 4-ABAH and H_2O_2. There was a similar extent of MP-11 inhibition found, and DMPO significantly prevented the inhibition.

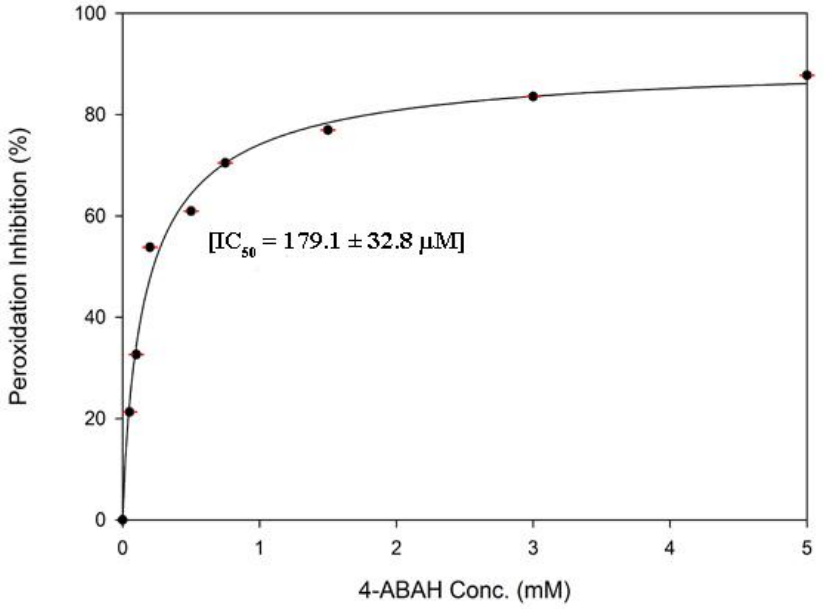

Fig.3.1 4-ABAH mediated dose-dependent MP-11 peroxidation inhibition curve. MP-11 (1 µM) was incubated at 35°C with 4-ABAH (various concentrations) in HPLC grade water for 30 min. The reaction was initiated by addition of guaiacol (0.600 mM) and H_2O_2 (0.600 mM) in ten folds dilute solutions of the above mentioned reactants. The reactions were scanned at each minute for 20 minutes. The peroxidase activity was measured by guaiacol assay at A_{450} until steady state kinetics was achieved. The experiment was repeated for maximum of 3 times and the mean ± standard error values are presented in the graph with Y error bars.

Table - 3.1 Peroxidase activity of MP-11 after incubation with 4-ABAH

Reactions	ΔO.D. $_{\lambda = 450\ nm}$
MP-11	0.184 ± 0.004
MP-11 + 4-ABAH	0.038 ± 0.001
MP-11 + DMPO + 4-ABAH	0.061 ± 0.001*
MP-11 + 4-ABAH + H_2O_2	0.043 ± 0.002
MP-11 + DMPO + 4-ABAH + H_2O_2	0.060 ± 0.002$^{\#}$

The concentrations of reactants were: MP-11 (1 µM), DMPO (100 mM), 4-ABAH (200 µM) and H_2O_2 (100 µM). All the reactions were incubated in HPLC grade water at 35˚C for 30 min prior to assay. Ten folds diluted samples were taken and added to guaiacol (0.6 mM) and H_2O_2 (0.6 mM). The absorbance tetraguaiacol was recorded as an endpoint spectrophotometrically at 450 nm after 10 min. This experiment was repeated for maximum of 3 times. Statistics (pairwise multiple comparison procedure – Student Newman Keuls Method)
(* $p<0.001$ compared to MP-11 + 4-ABAH; $^{\#}$ $p<0.001$ compared to MP-11 + 4-ABAH + H_2O_2).

3.2 MP-11 heme alteration by 4-ABAH

To gain further insight into the MP-11 inhibition by 4-ABAH, we performed MP-11 heme UV-Vis spectral scans. The collective spectra for maximum of 3 repetitions are represented below in each case. The spectrum presented in Fig. 3.2.1 shows the MP-11 heme absorbance maximum at 399 nm (Soret Band for MP-11). The scan was repeated after 5 min and 30 min at room temperature confirming that there is no change in the absorbance and hence MP-11 by itself was stable for at least 30 min. When H_2O_2 was incubated with MP-11 (Fig. 3.2.2) there was a slight decrease in the absorbance. However, after 5 and 30 minutes there was apparent heme degradation and no recovery to its original state. Similar findings showing MP-11 inactivation by H_2O_2 have been reported by others[41]. Moreover, in the presence of 4-ABAH alone (Fig. 3.2.3) MP-11 heme underwent a similar "bleaching" reaction as with H_2O_2 alone. However, this effect was accompanied by a shift in λ_{max} from 399 nm to 408 nm in the presence of 4-ABAH (Table 3.2). Shift in maximal absorbance was measured by (x,y) co-ordinates from the raw data. Heme modification of horseradish peroxidase by phenylhydrazine has also been reported to produce heme decay accompanied by a red-shift in the UV absorbance spectrum[37]. A greater shift in λ_{max} (415 nm) was detected in the reaction of MP-11 and 4-ABAH in presence of H_2O_2 (Fig. 3.2.4, Table 3.2). When DMPO was included in the reaction before the addition of 4-ABAH, there was attenuation of the decrease in the heme peak (Fig. 3.2.5).

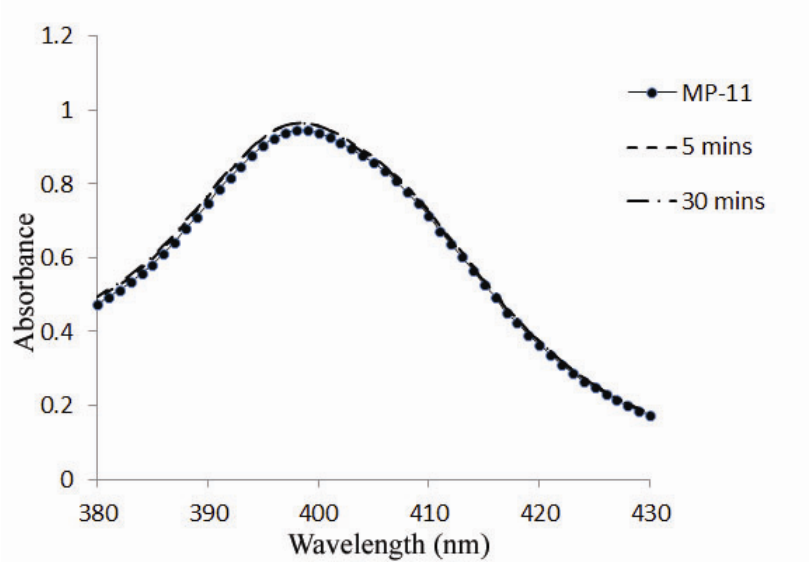

Fig. 3.2.1 Representative spectrum of MP-11 (1 µM), showing absorbance maxima (Soret Band) at 399 nm. There was no change in the maximal absorption at 5 mins & 30 mins.

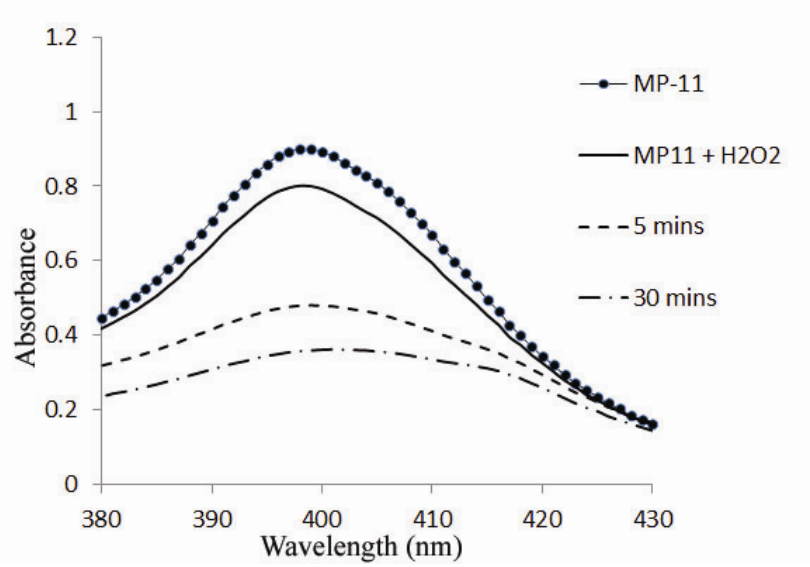

Fig. 3.2.2 Representative spectrum of MP-11 (1 µM) + H_2O_2 (100 µM). There was a reduction in the absorption immediately after the addition of H_2O_2 (possibly a Compound I intermediate), and apparent heme degradation 5 and 30 mins thereafter.

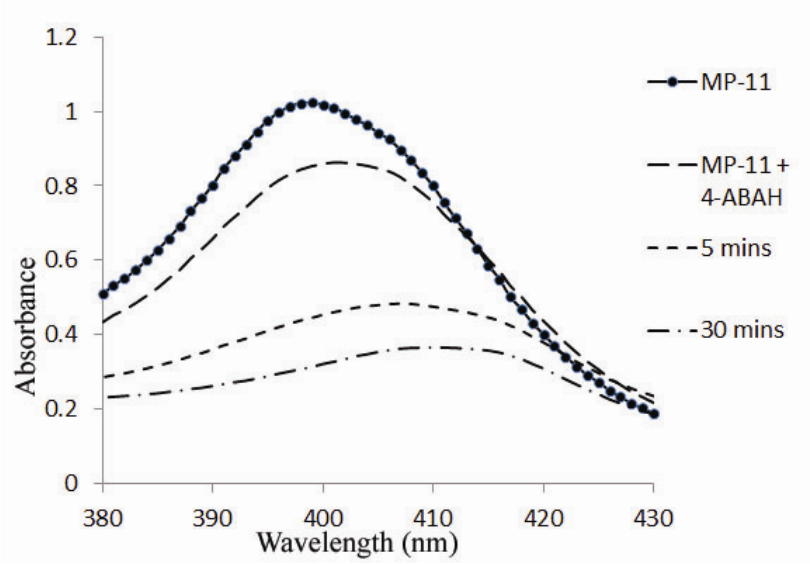

Fig. 3.2.3 Representative spectrum of MP-11 11 (1 µM) + 4-ABAH (200 µM). A spectral shift was observed upon addition of 4-ABAH. The absorption maximum shifted from 399 nm to 408 nm after 5 mins and further to 408 nm by 30 mins.

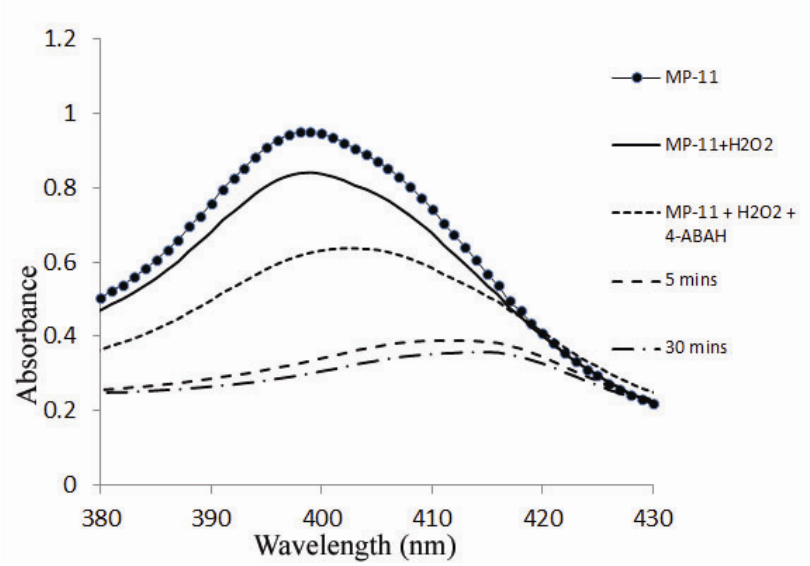

Fig. 3.2.4 Representative spectrum of MP-11 (1 µM) + H_2O_2 (100 µM) + 4-ABAH (200 µM). A further spectral shift was observed in this reaction at 415 nm. The maximal absorbance decreased 4-5 fold after 30 mins indicating heme degradation.

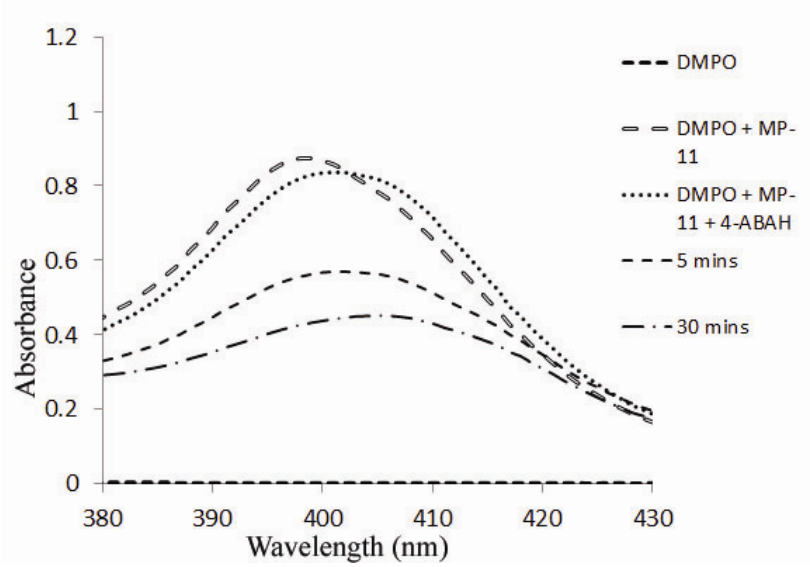

Fig. 3.2.5 Representative spectrum of DMPO (1 mM) + MP-11 (1 µM) + 4-ABAH (200 µM). A similar trend of spectral shift was observed here after the addition of 4-ABAH. After 30 mins, the absorption intensity was slightly higher than was observed in Fig. 3.2.3 suggesting a protective effect of DMPO.

Table. 3.2 Absorbance values for MP-11 spectra

	Absorbance				
Wavelength (nm)	MP-11	5 mins	30 mins		
400 ± 2	0.933 ± 0.014	0.952 ± 0.014	0.951 ± 0.015		
	MP-11	MP-11 + H_2O_2	5 mins	30 mins	
400 ± 2	0.894 ± 0.043	0.814 ± 0.028	0.453 ± 0.011	0.321 ± 0.011	
	MP-11	MP-11 + 4-ABAH	5 mins	30 mins	
400 ± 2	0.927 ± 0.011	0.815 ± 0.011	0.410 ± 0.011	0.325 ± 0.011	
412 ± 4	0.648 ± 0.097	0.0672 ± 0.082	0.419 ± 0.014	0.361 ± 0.006	
	MP-11	MP-11 + 4-ABAH	MP-11 + 4-ABAH + H_2O_2	5 mins	30 mins
400 ± 2	0.940 ± 0.012	0.833 ± 0.008	0.629 ± 0.008	0.340 ± 0.01	0.306 ± 0.008
414 ± 2	0.604 ± 0.054	0.566 ± 0.043	0.524 ± 0.024	0.386 ± 0.002	0.356 ± 0
	DMPO	DMPO + MP-11	DMPO + MP-11 + 4-ABAH	5 mins	30 mins
400 ± 2	0.003	0.863 ± 0.013	0.832 ± 0.006	0.566 ± 0.005	0.437 ± 0.007
407 ± 2	0.003	0.738 ± 0.04	0.785 ± 0.030	0.548 ± 0.015	0.447 ± 0.005

The absorbance value and concentration of the reactants mentioned in the table is obtained from spectrum (Fig. 3.2.1-5). The wavelength is reported as ± nm at absorbance maxima. The absorbance values for each reaction are reported as mean ± standard deviation. A shift in absorbance can be noted at various wavelengths in the reaction containing 4-ABAH.

3.3 Characterization of free radical metabolites of 4-ABAH and benzhydrazide (BAH) by ESR

ESR experiments were performed to characterize the identity of 4-ABAH free radicals involved in MP-11 inhibition. The reaction containing MP-11, 4-ABAH, and H_2O_2 in phosphate buffer of pH 7.3 generated an intense ESR spectrum using DMPO as the spin trap. The signals reported below are representative of DMPO-4-aminobenzoyl adduct and DMPO-benzoyl adduct accordingly. The splitting constants obtained were a^H = 18.56 G and a^N = 15.5 G (Fig. 3.3.1A). These splitting constants have been previously characterized as carbonyl radicals (R-CO$^{\bullet}$)[39]. To accurately identify the free radical species based on the hyperfine splitting constants, we simulated the spectrum producing a correlation coefficient = 0.997. The simulation was performed in WinEPR (Bruker Biospin) software. The signal intensity was reduced by 3-4 folds when MP-11 was not present in the reaction (Fig. 3.3.1B). Similarly, even less intense signals were detected when MP-11 and H_2O_2 were omitted (Fig. 3.3.1C). A mechanism of benzhydrazide carbonyl radical generation by HRP and that this carbonyl radical will form a covalent adduct with HRP heme has been proposed but not proven previously[5]. In Fig. 3.3.2, we show that in the absence of H_2O_2, both 4-ABAH and BAH generated less intense ESR spectra that appear to be identical based on the hyperfine splitting constants. Fig. 3.3.2A was shown in order to compare the relative intensity and hyperfine splitting constants of the spin-trapped radicals of 4-ABAH with BAH (Fig. 3.3.2C). In addition, these results show that addition of H_2O_2 was not required for oxidation of the inhibitors

(Figs 3.3.2 B & D). The hyperfine splitting constants for the BAH spin-adduct were a^N = 15.4 G, a^H = 18.0 G with correlation = 0.985. The a^H was different by 0.5 G which we propose is likely due to the absence of the *p*-amino group. It had been observed that the substituents on the benzene ring at *para* position to the amino group produced well-defined ESR spectra in case of aromatic amines[61]. Therefore, it can be noted from the above observations that MP-11 is required to catalyze the oxidation of 4-ABAH successfully.

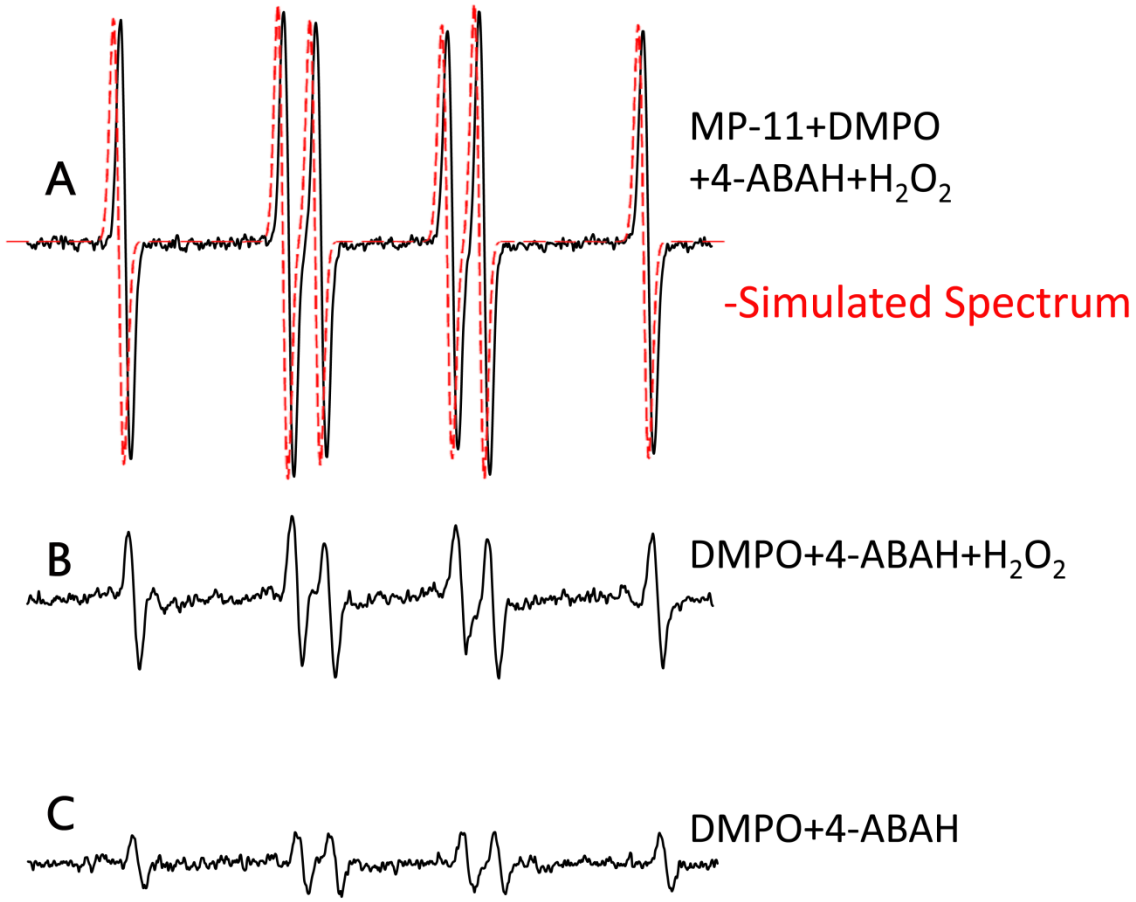

Fig.3.3.1 ESR spectroscopy of 4-ABAH in various controlled reactions in Chelex treated 0.1 M phosphate buffer pH 7.3. (A) Spectrum of MP-11 (100 μM), DMPO (100 mM) 4-ABAH (3 mM) and H_2O_2 (1.5 mM). The simulation of this spectrum (dashed line) corresponded to the following hyperfine splitting constant a^N = 15.5 G, a^H = 18.5 G with correlation = 0.997. (B) Same reaction condition as in (A) in the absence of MP-11. (C) DMPO (100 mM) and 4-ABAH (3 mM). Instrumental parameters were: operational frequency = 9.79 GHz, modulation = 100 kHz, modulation amplitude =0.4 G, power = 20 mW, gain = 60 dB, scan time = 163 s, time constant = 163 ms.

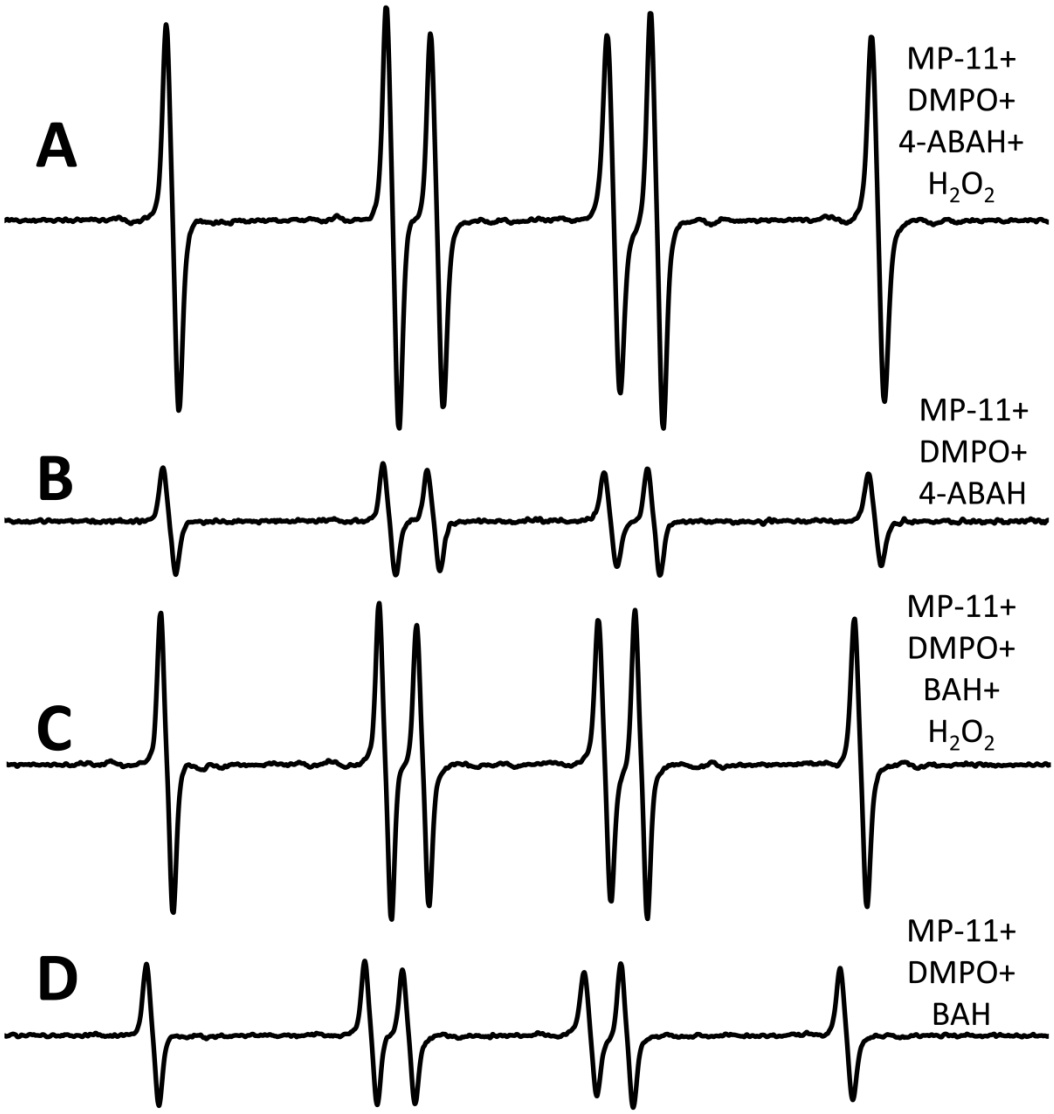

Fig. 3.3.2 ESR spectroscopy of 4-ABAH and BAH in Chelex treated 0.1 M phosphate buffer pH.7.3 with DMPO and H_2O_2. (A) ESR spectrum of MP-11 (100 µM), DMPO (100 mM) 4-ABAH (3 mM) and H_2O_2 (1.5 mM). (B) Same reaction condition as in (A) in the absence of H_2O_2. (C) ESR spectrum of MP-11 (100 µM), DMPO (100 mM), BAH (3 mM) and H_2O_2 (1.5 mM). (D) Same reaction condition as in (D) in the absence of H_2O_2. The hyperfine splitting constants for (C) and (D) were a^N = 15.4 G, a^H = 18.0 G with a correlation = 0.985. Instrumental parameters the same as indicated in Fig. 3.3.1

3.4 MALDI mass spectrometry

MALDI-TOF MS analyses of MP-11 reactions were carried out in HCCA matrix to characterize adduct formation. Fig. 3.4.1 shows the MALDI-TOF spectrum of MP-11. The mass spectrum of native MP-11 is m/z 1860.58 with secondary peaks [M + Na^+] and [M + K^+] approximately at m/z 1884 and m/z 1900 respectively. Fig. 3.4.2 represents the spectrum of native MP-11 that was incubated with 3 mM 4-ABAH for 30 minutes at 35 °C and then subjected to MALDI FTICR MS analysis. We observed three unidentified peaks (m/z of 1979.7787 (I), 1993.8049 (II) and 2112.8442 (III)). These peaks represent 4-ABAH adducts with MP-11 since we were not able to observe mass peaks in native MP-11 spectrum. The mass differences of each peak from the molecular ion peak (m/z 1860.7406) are 119.0374, 133.0643 and 252.1014 respectively. Table 3.4.1 shows the results of the high-resolution MS measurements where the elemental formulae were determined for unmodified MP-11 and the chemical adducts. Adduct I shows a change in elemental composition of C_7H_5NO, adduct II is a net addition of $C_7H_7N_3$ to the parent structure and adduct III could be a net addition of $C_{14}H_{12}N_4O$. We also performed similar experiments with benzhydrazide (desamino 4-ABAH congener) and observed parallel patterns of adduct formation (Fig. 3.4.4). Adducts I and IV correspond to the addition of 4-aminobenzoyl and benzoyl to MP-11 respectively. Adducts II and V have the same structural addition to MP-11 bearing in mind that BAH (adduct V) does not have *p*-amino group. These findings confirmed that the presence of p-amino group in 4-ABAH is not directly functional in its peroxidase inhibition activity.

Based on IC_{50} values, this was proved by structure activity relationship (SAR) of benzoic acid derivatives[4]. Furthermore, DMPO was included in the reaction with MP-11 and 4-ABAH (Fig. 3.4.3) to elucidate its role in the reaction. Adducts found in Fig. 3.4.2 were not found in this reaction, suggesting that the free radical metabolites of 4-ABAH preferentially reacted with DMPO, and that DMPO did not form a putative spin-adduct with MP-11 (protein radical). In other words, DMPO is effective in trapping free-radicals generated in the system and thereby restricts the 4-ABAH radical adduct formation with MP-11. Therefore, we were successful to obtain MP-11 and 4-ABAH adducts with their elemental formulae that could be responsible for MP-11 inhibition.

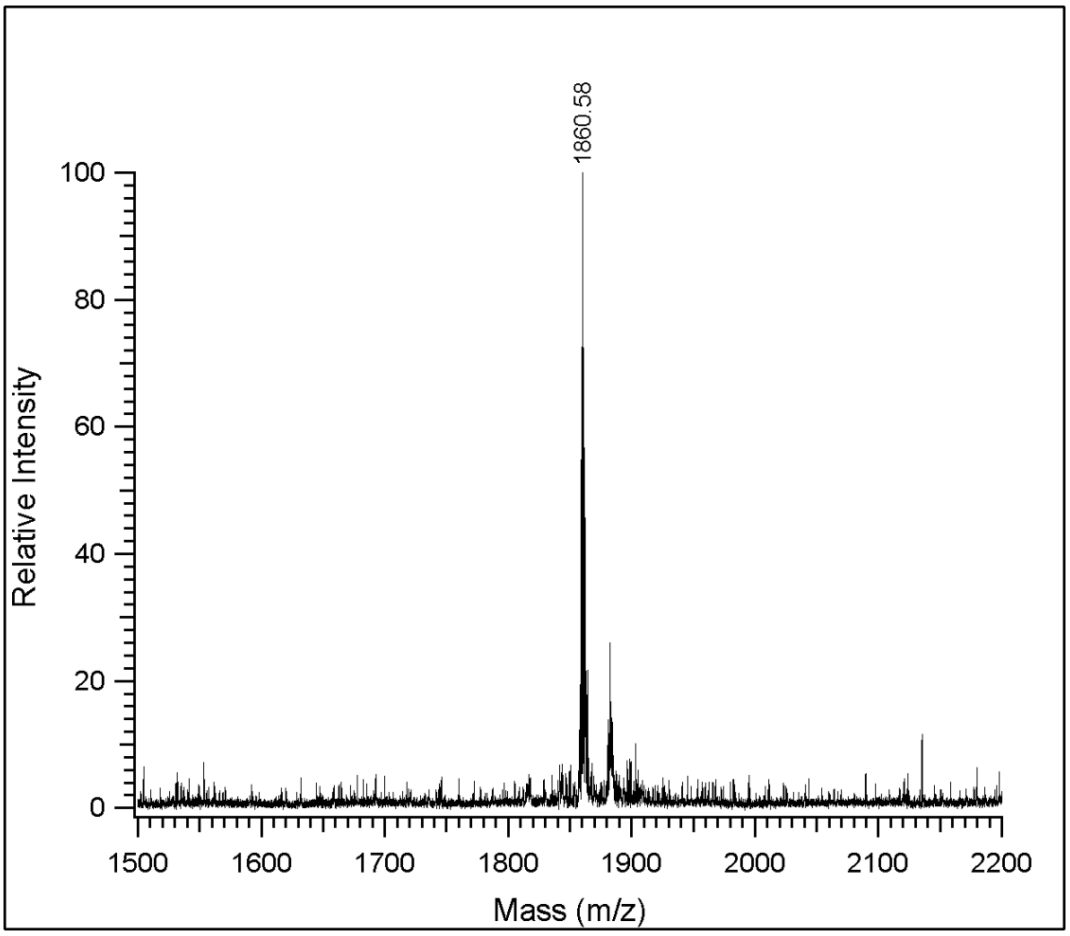

Fig.3.4.1 MALDI-TOF MS spectrum of MP-11 (100µM) after 30 minutes of incubation at 35 °C. The above spectrum shows the mass of unmodified peptide MP-11 at 1860.5 m/z.

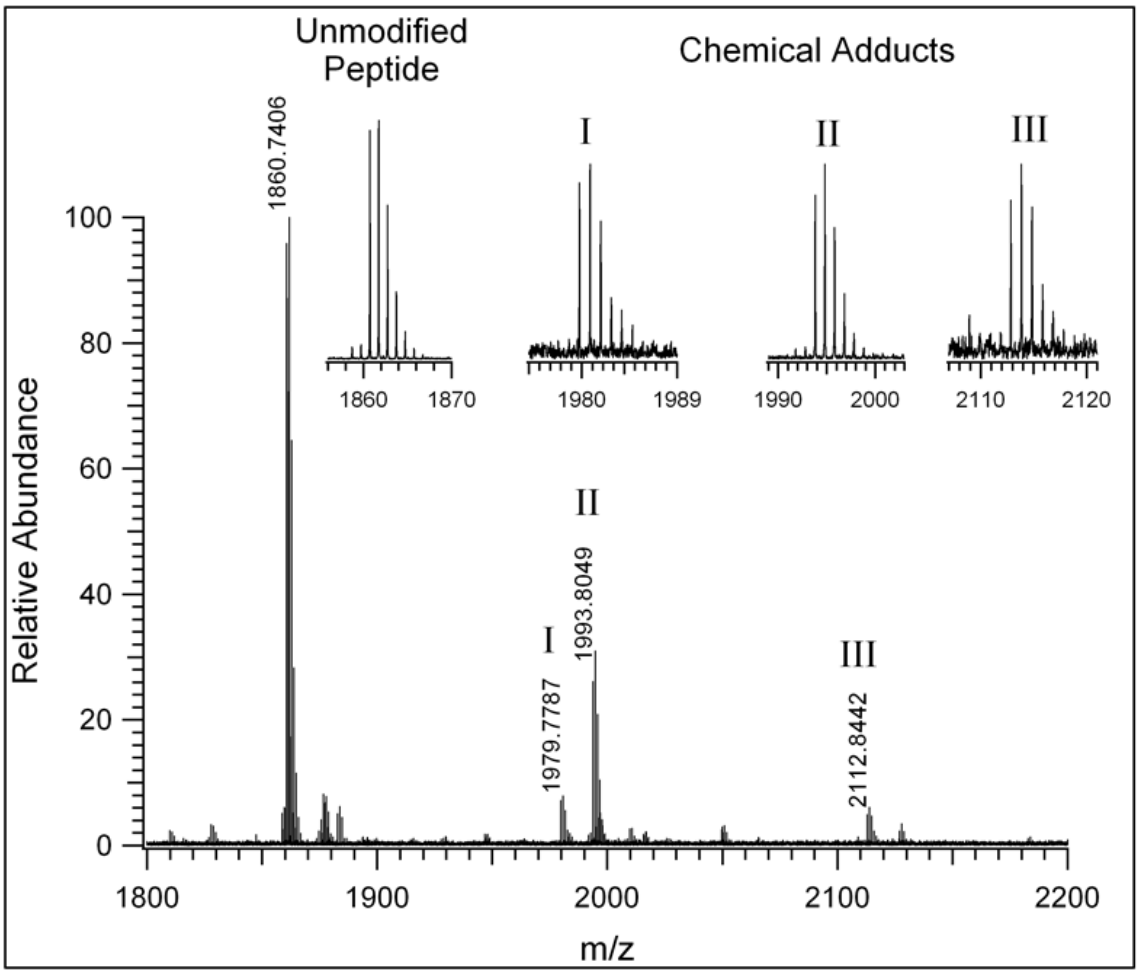

Fig.3.4.2 High-resolution MALDI FTICR MS spectrum of MP-11 (100 µM) and 4-ABAH (3 mM) at 30 min at 35 °C showing the formation of new peaks at m/z 1979 (I), 1993 (II) and 2112 (III).

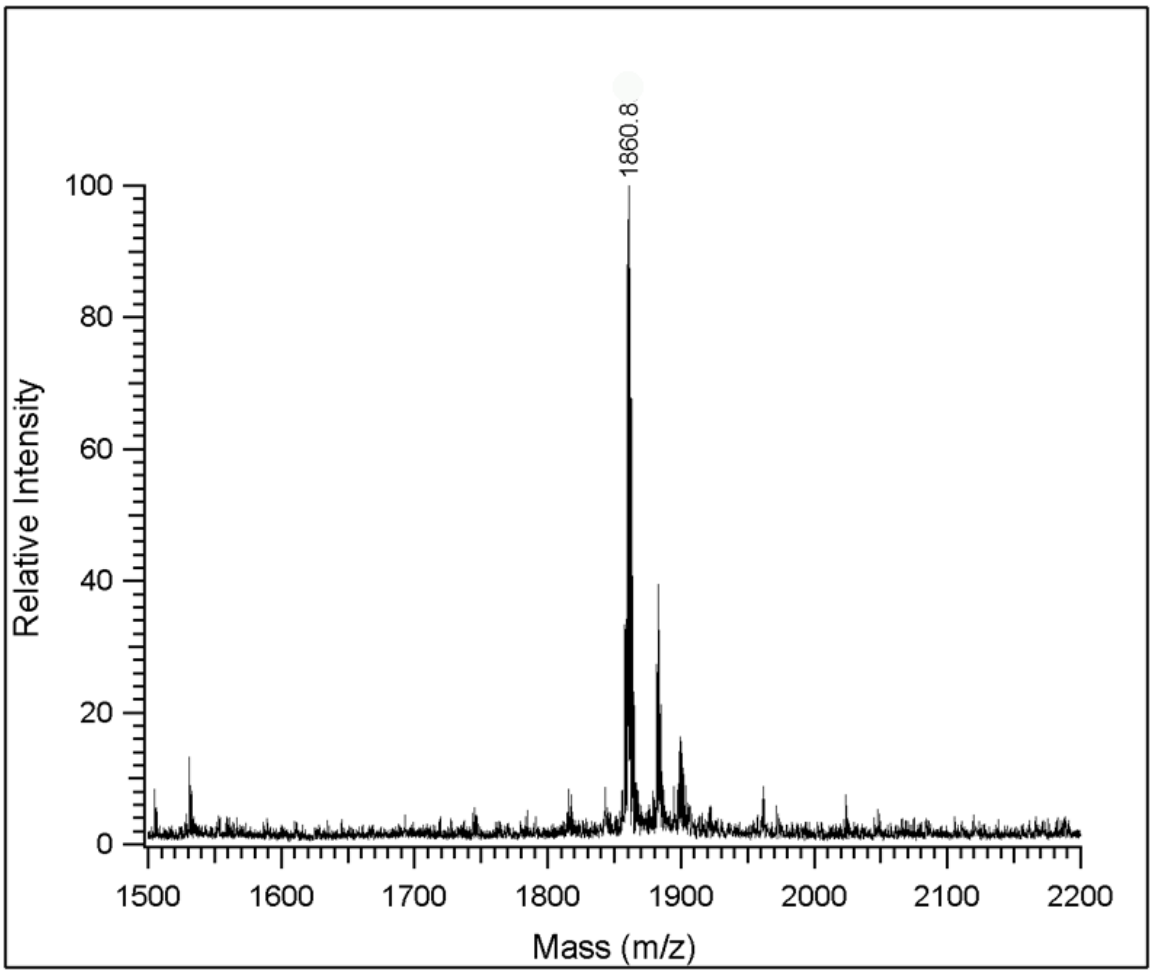

Fig.3.4.3 MALDI-TOF MS spectrum of MP-11 (100 µM) + DMPO (100 mM) + 4-ABAH (3 mM), incubated at 30 min at 35°C. This spectrum shows attenuation of the peak at m/z 1979(I) and 1994(II).

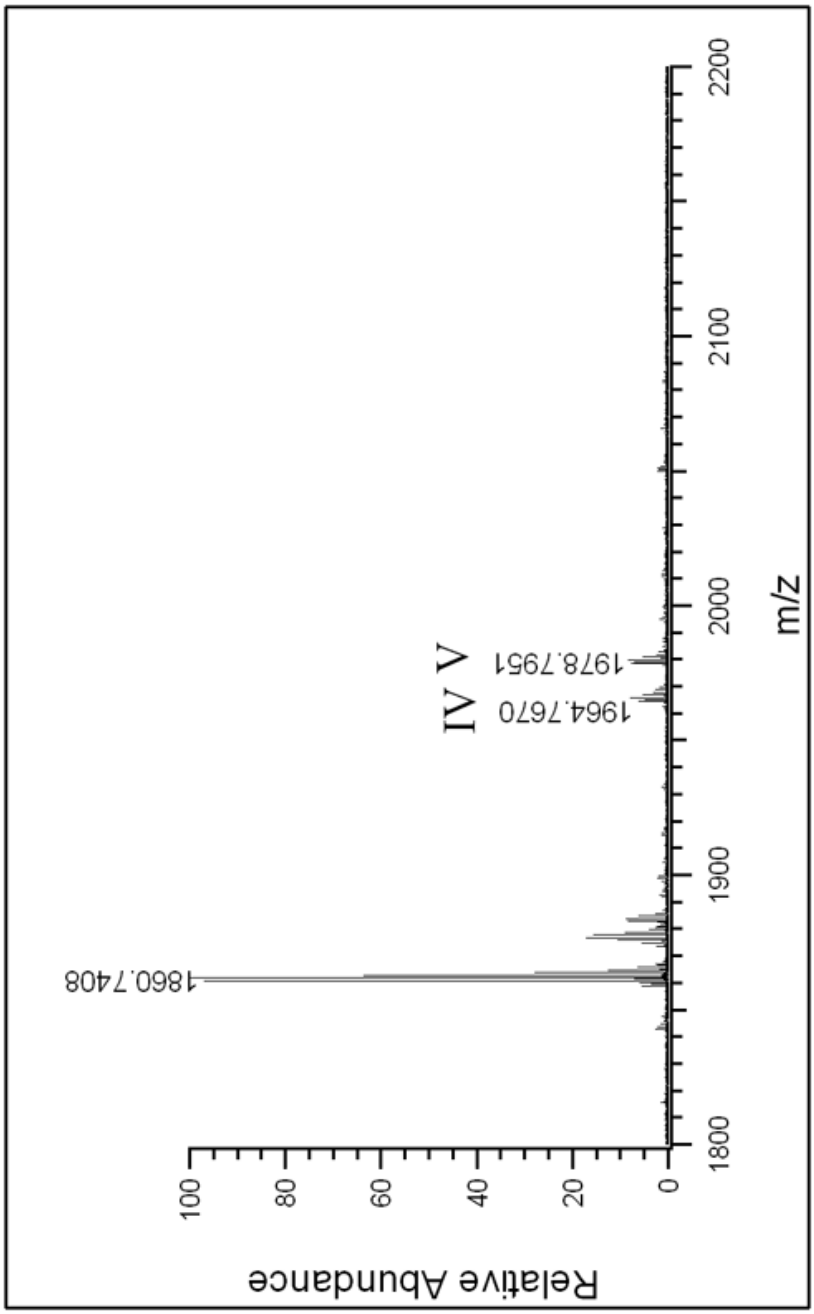

Fig.3.4.4. High-resolution MALDI FTICR MS of MP-11 (100 µM) + BAH (3 mM) In this case also, new adducts at m/z 1964 (IV) and 1978 (V) are observed.

Table 3.4.1 FTICR-MS analysis

Adduct	Chemical Formula	Theoretical (m/z)	Observed (m/z)	Error (ppm)
Unmodified peptide	$C_{84}H_{116}Fe_1N_{20}O_{21}S_2$	1860.7409	1860.7406	0.2
I	$C_{91}H_{121}Fe_1N_{21}O_{22}S_2$	1979.7780	1979.7787	-0.3
II	$C_{91}H_{123}Fe_1N_{23}O_{21}S_2$	1993.8049	1993.8049	0.0
III	$C_{98}H_{128}Fe_1N_{24}O_{22}S_2$	2112.8420	2112.8442	-1.0
IV	$C_{91}H_{120}Fe_1N_{20}O_{22}S_2$	1964.7671	1964.7670	0.1
V	$C_{91}H_{122}Fe_1N_{22}O_{21}S_2$	1978.7940	1978.7951	-0.5

FTICR-MS analysis of MP-11 (100µM) in presence of 4-ABAH (3 mM) and BAH (3 mM) using HCCA matrix with added $NH_4H_2PO_4$. The elemental analysis was performed for the above reaction after 30 min. This table represents the elemental composition of the various mass peaks observed in the high resolution spectrum (Fig. 3.4.2) together with their corresponding masses and error accounted in parts per million during the measurement. Adducts IV and V corresponds to Fig. 3.4.4 where BAH was used instead of 4-ABAH.

3.5 Western blots with MP-11

To obtain insight about the immunoreactivity of MP-11 and 4-ABAH adducts, we performed western blotting. Samples containing various reactants were run on specially formulated glycerol/SDS-PAGE gel since the molecular weight of the protein was about 1.8 kDa (Fig. 3.5.1). As shown, MP-11 alone or with H_2O_2 showed no anti-DMPO reactivity. However, the reactions containing MP-11 and 4-ABAH or MP-11, 4-ABAH, and H_2O_2 showed anti-DMPO (polyclonal) immunoreactivity. It could be that the reaction of MP-11 and 4-ABAH generates adducts that may exhibit cross reactivity with the antibody. Further, when DMPO was included in the reaction containing MP-11 and 4-ABAH, signal intensity was reduced as compared to 4-ABAH and MP-11. The reaction containing MP-11, 4-ABAH, and H_2O_2 produced the most intense bands, which appeared somewhat attenuated by the inclusion of DMPO. However, when POBN, another spin trap, was present with and without H_2O_2 in reactions containing MP-11 and 4-ABAH, signals were detected in both the reactions indicating the reactivity is identical regardless of presence of H_2O_2. These lead to additional experiments using monoclonal anti-DMPO antibody (Fig. 3.5.2). Consistent with the previous results (Fig.3.5.1), a similar pattern of immunorecognition was detected. Also we used anti-isonicotinoyl antibody (Fig.3.5.3) to detect 4-aminobenzoyl adduct by taking into consideration that it may have similar chemical characteristic as isonicotinic acid. Here too, use of DMPO (lane 6) was efficient in free-radical trapping and hence no signal was detected. These data confirmed that there is a definite 4-ABAH free-radical

intermediate is generated in the reaction cycle that is perceived as DMPO-nitrone adduct by anti-DMPO, regardless of anti-body class origin.

Surprisingly, chemiluminiscence signals were detected in a western blot where the membrane was either treated directly after transfer (Fig.3.5.4) or after blocking with gelatin (Fig.3.5.5). In both experiments, signals were apparent irrespective to the use of antibody. In former case, intense signals were noted indicating the direct interaction of MP-11 with luminol substrate as observed in lane 1 (Fig.3.5.4) which was not observed previously. Here, we had not used antibody for detection which implied that this interaction may not be immunogenic. In other experiment (Fig.3.5.5), when the membrane was blocked with gelatin, the signal intensity was comparably reduced. It can be assumed that the availability of MP-11 to interact with luminol in a blocked membrane is considerably lessened as observed in lane 1. However, in the reactions containing 4-ABAH, the signals intensity followed consistent pattern (Fig.3.5.1-3).

Extending the approach in a quest of detecting MP-11 reactivity with luminol, gelatin blocked membrane treated only with secondary antibody had further reduced the signal strength (Fig.3.5.6). However, the trend of immune recognition in this experiment was apparently similar as compared to previous western blots described here. Therefore, alkaline phosphatase based detecting system was used to verify the formation of true MP-11 and 4-ABAH adduct and also to limit the peroxidase and substrate mediated chemiluminscence. MPO-DMPO adduct (lane 1) from cell lysate was used as positive control to confirm the functionality of the alkaline phosphatase based detection (Fig 3.5.7). No

immunorecognition were observed in reactions that included MP-11(lane 3-7). From this experiment, it was confirmed that the signals observed the previous western blots were due to the chemical reactivity between MP-11 and luminol substrate. Further, the inclusion of 4-ABAH, H_2O_2 and DMPO in the reactions mediated differences in signal intensity.

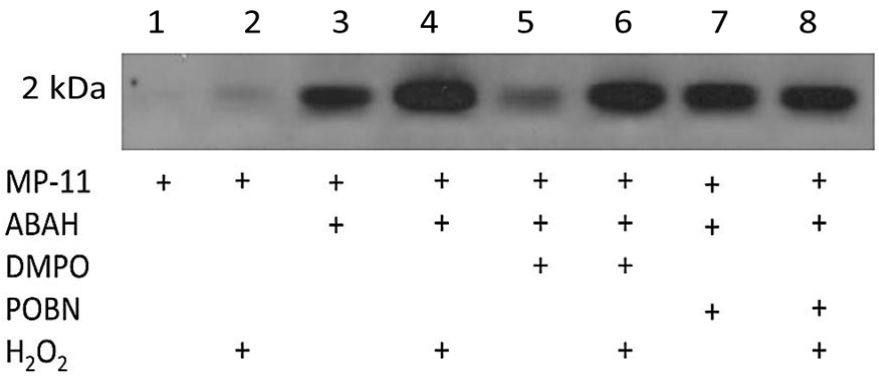

Fig.3.5.1 Representative western-blot of MP-11 with 4-ABAH in presence of spin traps DMPO and POBN using polyclonal anti-DMPO antibody. MP-11 (100 µM) was incubated with DMPO (100 mM), POBN (100 mM), 4-ABAH (3 mM) and H_2O_2 (1.5 mM) in various reactions at 35 °C for 30 minutes prior to loading. Anti-DMPO recognition was observed in lanes 3 and 4 which did not contain DMPO. DMPO (lane 5) attenuated the reaction in lane 3. The addition of H_2O_2 (lane 6) however, increased detection in lane 6. Addition of the spin trap POBN did not attenuated anti-DMPO binding (lanes 7 & 8). Results are described further in the text. This experiment was repeated for a maximum of 15 times.

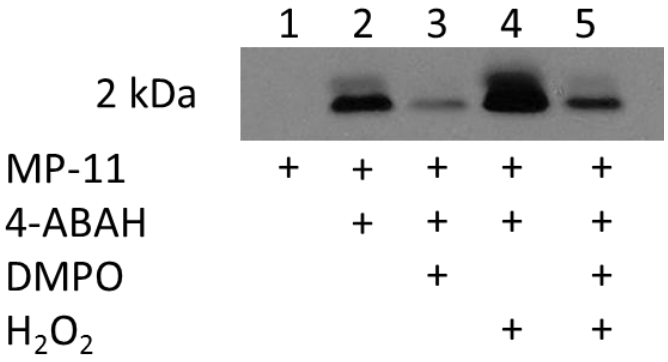

Fig.3.5.2 Representative western-blot of MP-11 with 4-ABAH in presence of spin traps DMPO using monoclonal anti-DMPO antibody. MP-11 (100 µM) was incubated with DMPO (100 mM),4-ABAH (3 mM) and H_2O_2 (1.5 mM) in various reactions at 35 °C for 30 minutes prior to loading. Anti-DMPO recognition was observed in lane 2 and 4 which did not contain DMPO. DMPO attenuated the reaction in lane 3 and 5. The addition of H_2O_2 (lane 4) increased immunorecognition. This experiment was repeated for a maximum of 5 times.

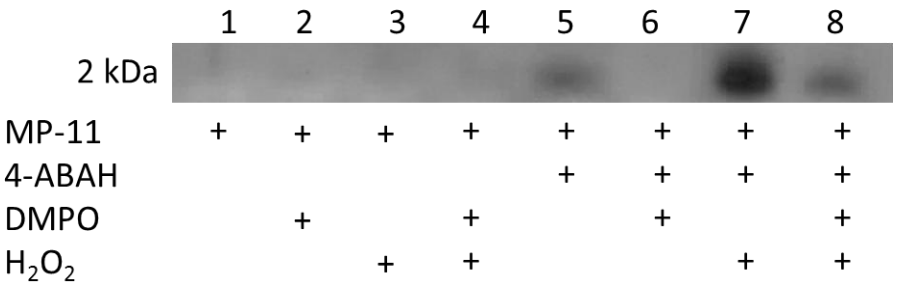

Fig.3.5.3 Representative western blot of MP-11 and 4-ABAH using rabbit anti-Isonicotinoyl antibody to assess if it can recognize 4-aminobenzoyl intermediate generated in the reaction. The reaction condition was same as mentioned in Fig.3.5.1. Lane 1, 2, 3 and 4 were used as negative control. Anti-isonicotinoyl recognition was observed in lane 5, 7, 8 and not in lane 6. This experiment was repeated for a maximum of 3 times.

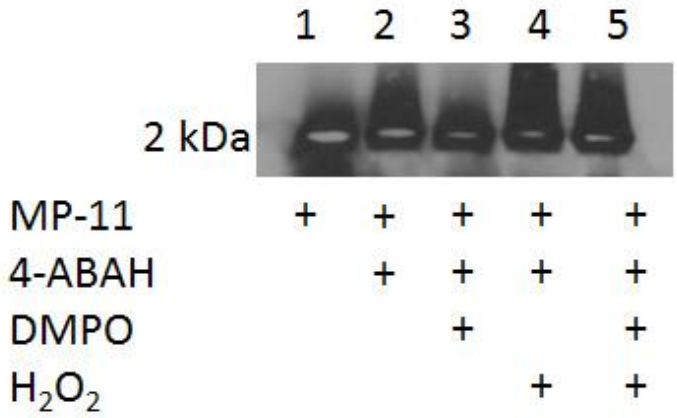

Fig.3.5.4 Western blot of MP-11 with 4-ABAH in the presence of spin trap DMPO. MP-11 (100 µM) was incubated with DMPO (100 mM),4-ABAH (3 mM) and H_2O_2 (1.5 mM) in various reactions at 35 °C for 30 minutes prior to loading. The membrane was developed with luminol after transferring the protein from gel. This blot suggested that there is a definite interaction of MP-11 with chemiluminiscence substrate containing luminol. This experiment was repeated for maximum of 2 times.

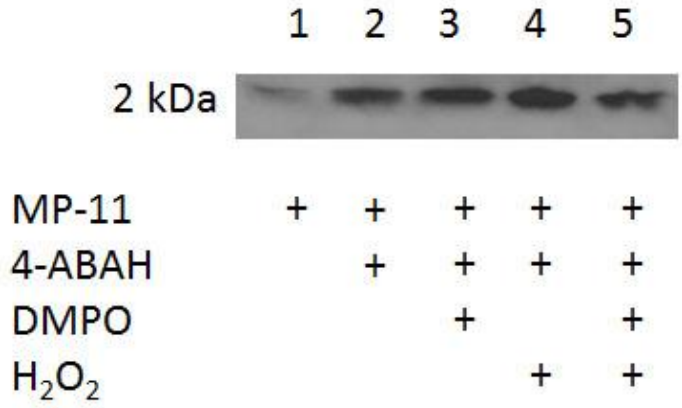

Fig.3.5.5 Western blot of MP-11 with 4-ABAH in the presence of spin trap DMPO. MP-11 (100 µM) was incubated with DMPO (100 mM),4-ABAH (3 mM) and H_2O_2 (1.5 mM) using same conditions as above. The membrane was developed with luminol immediately after blocking step. The band intensity was reduced as compared to fig.3.5.4. This blot suggested that MP-11 reactivity with luminol decreases in case of blocked membrane.

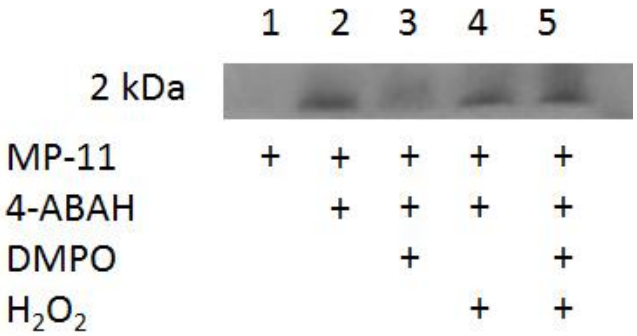

Fig.3.5.6 Representative western blot of MP-11 with 4-ABAH in the presence of spin trap DMPO. MP-11 (100 µM) was incubated with DMPO (100 mM),4-ABAH (3 mM) and H_2O_2 (1.5 mM) using same conditions as above. The membrane was developed with luminol after incubation with secondary goat anti-Rabbit IgG. The band intensity was further reduced as compared to fig.3.5.5. The use of secondary antibody results into detection of 4-ABAH reacted MP-11. This experiment was repeated for a maximum of 2 times.

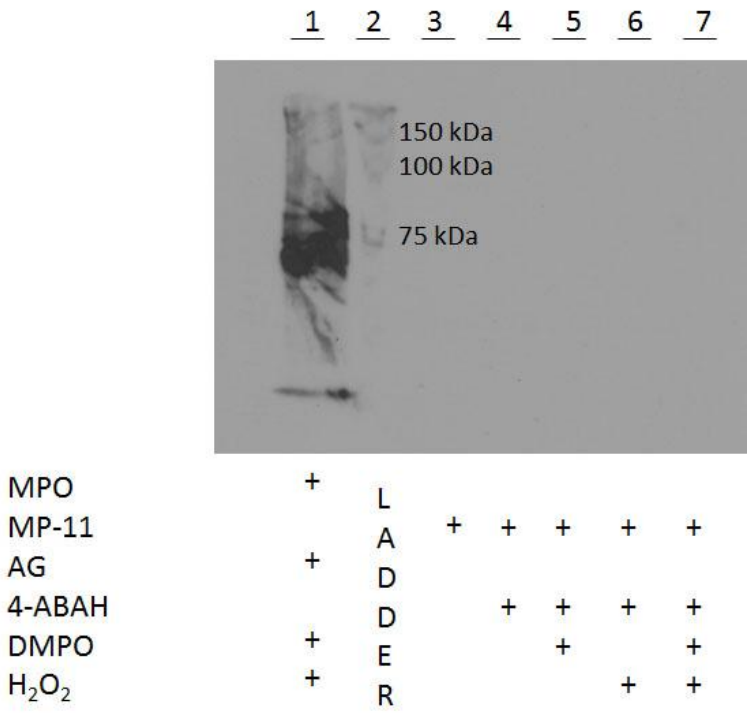

Fig.3.5.7 Polyclonal anti-DMPO western blot of MP-11 and 4-ABAH, developed by alkaline phosphatase (AP) as chemiluminiscence substrate. Lane 1 is loaded with the sample containing MPO to assess AP detection capability. This sample is aminogluthetimide (AG) treated HL-60 cell lysate, containing DMPO as a spin trapping agent. However, in lane 3-7 no anti-DMPO recognition is observed indicating that there is no true DMPO adduct formation in the reaction detectable by anti-DMPO antibody. Molecular weight marker is fairly visible.

Chapter 4 - Discussion

4.1 Discussion

There has been a vast amount of information concerning MPO inhibition by 4-ABAH[4,40,62]. However, we have provided a detailed insight into the mechanism of inhibition. We have been successful to prove that 4-ABAH can inhibit MP-11 and a portion of this inhibition can be reversed by DMPO (ref. 3.1-3.2). We hypothesized that free radical mechanism was involved in this inhibition. Also, it was assumed that there were free radical intermediates involved in the reactions between hydrazides and peroxidases[5,39,40]. In addition, it was mentioned that these intermediates were capable of forming adducts with peroxidase heme. Using ESR, we have succeeded in determining the free-radical identity responsible for this effect. Apparently, a catalyst was not required in this reaction (ref. 3.2-3.5), which differs from the inhibition of myeloperoxidase[40]. We identified MP-11 and 4-ABAH adducts along with their elemental composition using MALDI-TOF (ref. 3.4).

4.1.1 Atypical peroxidase behavior of MP-11 affecting 4-ABAH reactivity

Hydrogen peroxide is a prerequisite for Compound I formation from MPO which subsequently would react with substrates. One of the possible reasons behind the specific and atypical MP-11 peroxidase reactivity could be due to the distal site of the porphyrin. Unlike other peroxidases, MP-11 has open distal site that could perhaps help the substrate to directly react with the porphyrin[43]. This could eventually lead to Compound II formation without any involvement of hydrogen peroxide. Furthermore, a transient intermediate [Fe^{+3}-O_2H^-] formation has been suggested between MP-8 and H_2O_2 which reverts to a Compound I state.

Uncommon in other peroxidases, aggregation is a property that has been attributed to microperoxidases in aqueous solutions. Ionization of histidine was observed as a result of aggregation and this could add up to such uncommon peroxidase reactivity[47]. Also, it may be due to auto-oxidation of the hydrazide which produced a low flux of H_2O_2 that was sufficient to metabolize 4-ABAH. Earlier, suicidal inactivation of MP-11 was reported with the use of hydrogen peroxide[45]. Unlike that study, we had used the concentration of hydrogen peroxide that was sufficient to initiate and enhance 4-ABAH reactivity towards MP-11. We had also confirmed that the peroxidase activity of MP-11 with hydrogen peroxide was retained even after 30 minutes (Table 3.1). Therefore, to summarize these findings it can be said that either microperoxidases can act on a typical peroxidase pathway through the formation of Compound I and II analogues or it can follow degradative pathway involving irreversible attack of substrate on the porphyrin.

The effectiveness of 4-ABAH in comparison to various benzoic acid hydrazide derivatives for MPO inhibition was proved via measuring IC_{50} for peroxidation by ABTS[40]. We followed a similar approach for MP-11 by measuring its peroxidase activity using guaiacol assay (Fig. 3.1). Unlike MPO, a huge difference in the IC_{50} i.e. MP-11~ 179 μM and MPO ~ 2.2 nM[40] was found. This can be accounted as the limitation in using MP-11 for modeling peroxidase based oxidation reactions. This low reactivity of MP-11 could be due to the presence of primary structure and number of amino acids as compared to MPO that has tertiary globin structure.

4.1.2 ESR characterization of 4-ABAH radicals

We were successful in characterizing the free radical species that may be involved in MP-11 inhibition (Fig. 3.3.1-2). From the hyperfine splitting constants and simulation spectra, we confirmed that MP-11 catalyzes the oxidation of 4-ABAH to form 4-aminobenzoyl radical (C-centered radical). An agreement can be established between the splitting constants of DMPO spin adduct for isoniazid in HRP system[39] and the splitting constants of DMPO/4-aminobenzoyl adduct that we obtained in MP-11 system. In addition, we have characterized a similar adduct using BAH in MP-11 system (Fig. 3.3.2). However, it has been previously viewed that isoniazid auto-oxidizes in the presence of metals or by hemin[63]. Although our buffer was Chelex-100 treated with 1 mM DTPA there may have still been trace metals present or that MP-11 itself could oxidize 4-ABAH directly. It has been proposed that the formation of heme adducts in myoglobin proceeds via alkyl hydrazines autoxidation to an alkyldiazenes[64]. Further, ESR spectrum shows a detectable radical, albeit lower in intensity than that with the addition of H_2O_2. However, we attempted to detect H_2O_2 production indirectly using O_2 electrode (by O_2 production with catalase in the reaction) but were unsuccessful (data not shown). Interestingly, with both 4-ABAH and BAH the absence of H_2O_2 still resulted in significant spin trapping of the 4-aminobenzoyl or benzoyl radical metabolites, respectively.

Besides, an interesting observation in relation to the free radical formation was viewed. The use of DTPA in the phosphate buffer composition led to the decrease in the intensity of the ESR spectrum of 4-ABAH-DMPO adducts. A

similar observation was reported for hydrazines/HRP using spin-trap POBN. Low yields of alkyl-POBN adduct were obtained that may be due to the presence of DTPA which caused slow oxidation of the hydrazines[65]. Further in phenylhydrazine, use of EDTA (ethylenediaminetetraacetic acid) inhibited the oxidation as measured in terms of absorbance changes[66].

Although, the identity of the one of the free-radical intermediates was confirmed, the complete characterization is still to be executed. From the splitting constants, it was identified that 4-ABAH metabolized to a carbonyl (4-aminobenzoyl) radical. However, the other half of the molecule i.e. hydrazine moiety which must have been generated as a product of 4-ABAH breakdown was not detected. It is described that hydrazine has property to reduce DMPO and form DMPO-H adduct[67]. In other words, this will lead to the evolution of nitrogen/ammonia gas in the form of bubbles but was not observed in these specific reactions.

4.1.3 Benzoic acid hydrazides adducts with MP-11

We detected three covalent adducts having the elemental difference from native MP-11 of $+C_7H_5NO$ (119.0374 m/z), $+C_7H_7N_3$ (133.0643 m/z), and $+C_{14}H_{12}N_4O$ (252.1014 m/z) for 4-ABAH (Fig. 4.1.2) which were not observed in the native MP-11 spectrum (Fig. 4.1.1). Also, we found that the covalent adducts of BAH were identical once we accounted for the *p*-amino group of 4-ABAH. Based on these mass differences, we believe that we have evidence that there is the addition of 4-aminobenzoyl to MP-11 (adduct I, fig. 4.1.2). One of the mechanisms proposed earlier describes the formation of benzoyl-heme (HRP)

adduct that may have a structural similarity of adduct I (4-aminobenzoyl-MP-11 heme)[5]. As per this mechanism, the reaction will proceed via elimination of di-imide (NH=NH) to form benzoyl free-radical. This study was performed on heme isolated from HRP. The benzoyl-HRP heme adduct had a mass m/z 720 constituting HRP-heme (m/z 616) and benzoyl moiety (m/z 104). In our study, we found that there is covalent adduct formation between MP-11 and BAH (adduct IV, Fig. 3.4.4) that has a mass m/z 104.02. We propose that there could be a dehydration reaction that occurs for adduct II since the loss of the carbonyl oxygen and adduct formation involving the carbonyl carbon is a possible means to account for the mass change. The reaction mechanism involved will require future research, but appears significant since adduct II was the most abundant mass.

Furthermore, our findings show that there is no absolute requirement, *per se*, of *p*-amino group in 4-ABAH to activate the benzhydrazide moiety. Although, the 4-amino group is not required, it increases the inhibitory potential of 4-ABAH as observed in study comparing the inhibition ability of various benzoic acid derivatives. The electron donating nature of 4-NH_2 group provides the electronegativity and hence more affinity towards the peroxidases[4]. BAH, the desamino congener also showed a similar pattern of binding and adducts formation in mass spectrometry studies, where the mass difference between it and 4-ABAH was due to the amino group.

In this study, DMPO exerted a different action than simply spin trapping (Table 3.1). Indeed our mass spectrometry data showed the attenuation of peaks

formed by 4-ABAH with MP-11 when DMPO was added to the reaction (Fig. 3.4.3). The protective effect of DMPO has not been reported in the past. This protective effect of DMPO on MP-11 peroxidase activity suggests that the 4-ABAH-derived free radical was involved in inactivation of the enzyme. There was not complete protection of activity which suggests that the 4-aminobenzoyl radical more favorably reacted with heme than DMPO.

4.1.4 Immunoreactivity of 4-ABAH adducts

Another method by which we ascertained the covalent modification was through the application of western blots for MP-11. Successful transfer and immunoblotting of MP-11 was shown here for the first time. These immuno-spin trapping studies provided unexpected, yet informative data. First of all, these studies were performed on the premise that a protein radical could be formed (by 4-ABAH free radical metabolite oxidation of MP-11) then trapped with DMPO to produce a protein-DMPO adduct. The mass spectrometry evidence (Fig. 3.4.2) shows that there is a covalent interaction between a metabolite of the inhibitor and MP-11. It is likely that there is resemblance between the original antigen (DMPO-protein adduct) and (MP-11-4-ABAH adduct) which is recognized by anti-DMPO antibody. However, the antibody specificity for DMPO-protein adduct has been demonstrated in numerous studies[50]. This was established through competition experiments. Original antigen (DMPO-octanoic acid) and myoglobin-DMPO antigen were probed for detection by anti-DMPO antibody. In addition, they concluded that the affinity of anti-DMPO for DMPO binding is lesser than the concentration of DMPO (~100mM) used in the reaction. Instead our findings

showed that in the absence of DMPO, anti-DMPO detection occurred with particular prominence in samples containing 4-ABAH and MP-11 (Fig. 3.5.1). These results instigated further investigation using monoclonal anti-DMPO antibody which had a similar trend of reactivity (Fig. 3.5.2). In our previous experiments, we concluded the formation of 4-aminobenzoyl adduct with MP-11 (ref 3.3-3.4). Therefore we applied the use of an anti-isonicotinoyl antibody in lieu of anti-DMPO to detect possibly 4-ABAH adducts (Fig. 3.5.3). Following the trend of the results, there was no recognition of MP-11 alone or with MP-11 and H_2O_2 even though the latter resulted in heme degradation. These lead us to conclude that the anti-DMPO antibody is recognizing adducts between 4-ABAH and MP-11 that could have same binding domain as DMPO-nitrone adduct. In contrast, the presence of DMPO was able to significantly attenuate this recognition perhaps due to trapping of 4-ABAH free radical metabolites. The dispute was resolved with the use of POBN which had little effect on anti-DMPO detection suggesting that POBN played a small part in radical scavenging that affects antibody recognition.

In a quest to demystify the strange antibody reactivity, the experiments performed with and without antibody overshadowed the peroxidase behavior in a peroxidase-based detection system. It was deceptive that MP-11 reacted with luminol, a constituent of chemiluminiscence detection to produce an intense artefactual signal. Moreover, the use of alkaline phosphatase detection system confirmed true MP-11 reactivity since no bands were observed. Interestingly, there were differences in signal intensity of the western blots developed at various

phases of the procedure. The contrasting nature of results represented in [Fig. 3.5.4-6] emphasizes the fact that blocking the membrane as well as the use of antibody restricts the availability of free peroxidase in the reaction perceived via band intensity. In fact, microperoxidases have been used by Yamashoji to enhance the luminescence produced by H_2O_2-luminol system[68]. Furthermore, the use of fluorescent labeled antibody can be ruled out in this system since the signals of MP-11 and luminol are observed. It can be said that the role of antibody in these experiments is limited (ref. 3.5). We were able to observe signals in the samples that contained 4-ABAH while no signals were detected in samples containing MP-11 alone or MP-11 with H_2O_2 and/or DMPO. We tried to quantify the protein loading by staining the gel with coommassie blue. However, we were not successful in staining the gel to detect the proteins possibly due to the glycerol in the gel composition which may have resisted the stain.

One of the probable explanations for the reactivity differences in the samples containing MP-11 and 4-ABAH towards luminol is due to structural similarity of 4-ABAH and metamitron (Fig. 4.1.1). Metamitron, a triazinone herbicide has (-$CONRNH_2$) while with 4-ABAH (-$CONHNH_2$). MP-11 and luminol mediated reaction in chemiluminiscence detector is used for quantitative detection of pollutants like metamitron[69]. Therefore, MP-11 has been used indirectly for detection of metamitron. These findings can be expanded further in a future study.

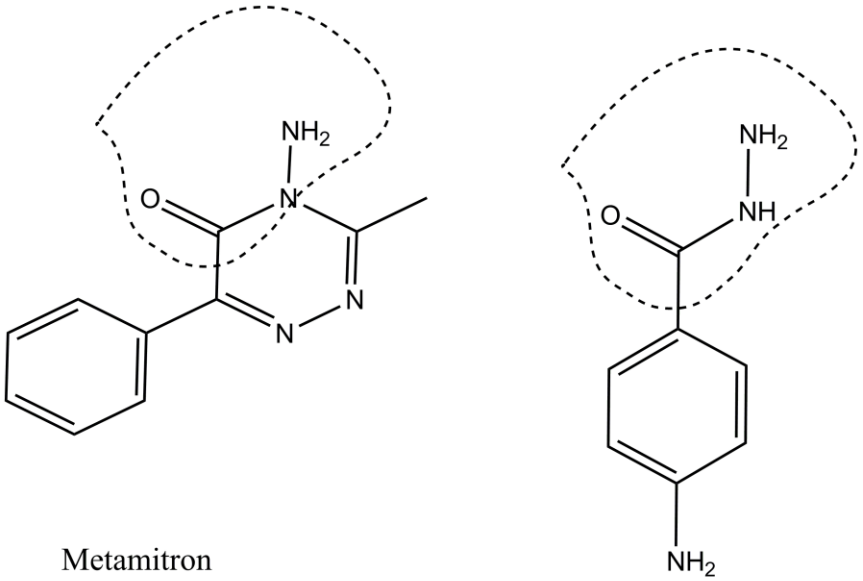

Fig.4.1.1 Structural comparison of metamitron and 4-ABAH. Similarity in side chain is indicated by dotted lines

4.2 Conclusion

We have successfully concluded the reactivity mechanism of MP-11 with 4-ABAH (Fig. 4.2). It was established that 4-ABAH mediated inhibitory action on MP-11 which includes inhibiting heme and peroxidase activity (ref. 3.1-3.2). We demonstrated the involvement of free radical mechanism in the MP-11 inhibition (ref 3.3). Further, the free radical intermediates responsible for enzyme inhibition were characterized in ESR (DMPO-4ABAH adduct, Fig. 4.2). The primary radical (Unstable adduct, Fig. 4.2) was not detected. Based on the splitting constants, 4-aminobenzoyl radical formation was concluded.

Moreover, 4-ABAH was shown to form covalent adducts with MP-11 that were associated with catalytic inhibition of the enzyme. The structural identity of Adduct I (Fig. 4.2) has been confirmed in ESR as well as MALDI MS elemental analysis, while Adduct II (Fig. 3.4.2 & 4.2) is yet to be characterized. Based on the mass differences, we concluded that Adduct III (Fig. 3.4.2 & 4.2) is a net addition of Adducts I & II. MP-11 appeared to have direct interaction with luminol that has considerable effect in detection of 4-ABAH adducts by western blotting (Fig. 3.5.1-6). Although DMPO is a spin trapping agent, it had partial free radical scavenging effect (Table 3.1, Fig.3.2.5 & 3.4.3). The presence of H_2O_2 accelerated MP-11dependent oxidative catalysis of 4-ABAH (Fig. 3.3.1-2). In conclusion, 4-ABAH was shown to inhibit MP-11 via a free radical mechanism and that free radical metabolites were shown to form covalent adducts with MP-11.

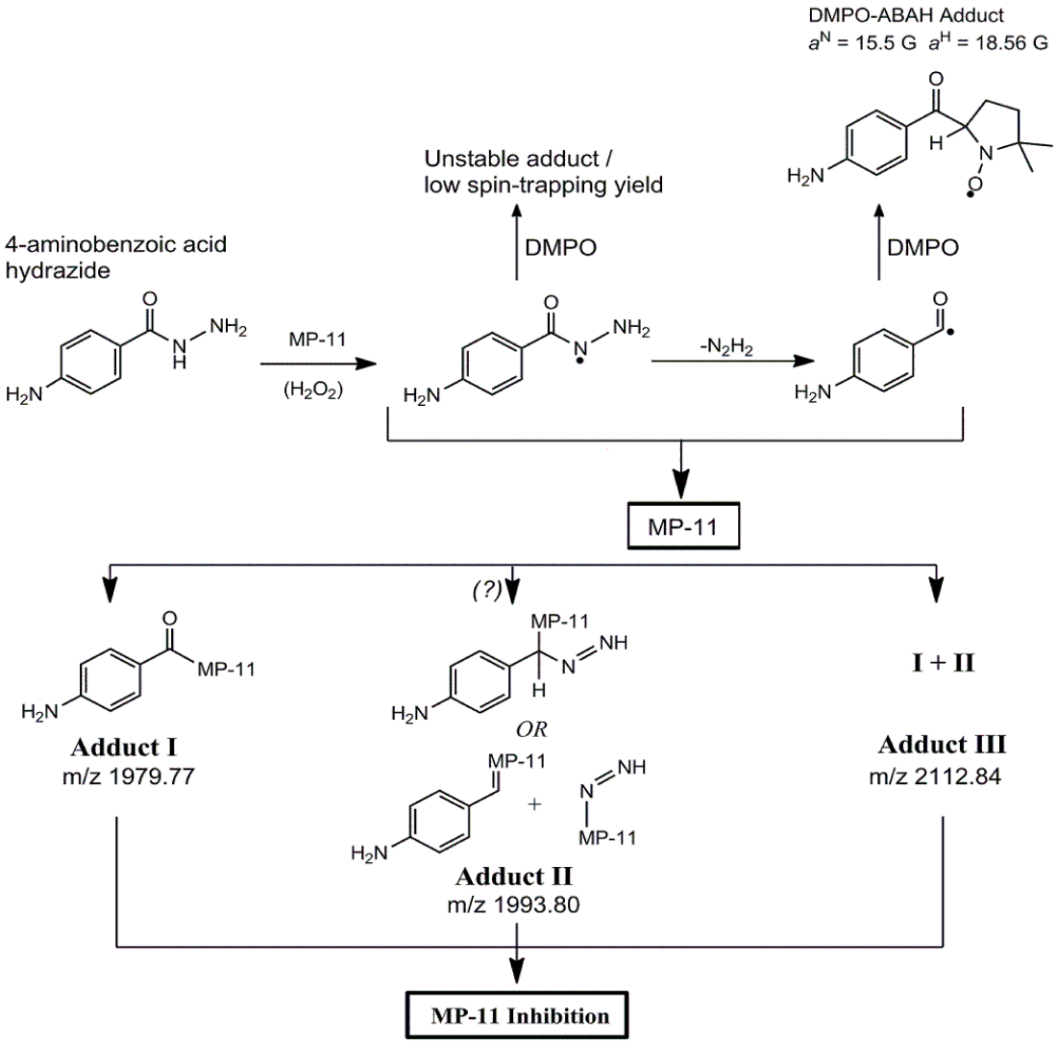

Fig. 4.2 Proposed mechanism of 4-ABAH free-radical metabolite generation in the presence of MP-11. Reaction of MP-11 with 4-ABAH in presence/absence of H_2O_2 can lead to 4-ABAH radical metabolites to cause MP-11 inhibition. The 4-aminobenzoic acid hydrazyl radical is postulated to form based on the exact masses obtained from high resolution MALDI MS. The 4-aminobenzoyl radical was formed from the latter radical, trapped with DMPO and detected by ESR. Further, one or both of these radical metabolites can cause heme modification by covalently binding with MP-11 heme (adduct I, adduct II, & adduct III). The structure of adduct II is proposed and further investigations are required. However we speculate that the 4-aminobenzoic acid hydrazyl radical undergoes dehydration and radical rearrangement upon binding to MP-11, or proceeds via Schiff base formation with hydrazyl addition (adduct II). Adduct III corresponds in mass to be the addition product of adduct I & II with MP-11.

4.3 Future Study

In our study, we confirmed the presence of free radical mechanism with hydrazides and also free radical species involved in MP-11 inhibition. It will be worthwhile to identify if the same free radicals are responsible for MPO inhibition. These experiments can be performed on isolated MPO or on HL-60 cells (human promyelocytic leukemia cells. In addition to MPO inhibition by 4-ABAH free radical intermediates, it is likely that hydrazides can lead to protein free radical formation. DMPO can be used in this study to spin trap and detect the protein free radicals using anti-DMPO sera by western blotting or ELISA. We have not characterized the Adduct II of 4-ABAH and MP-11 by ESR or MALDI-MS analysis. Alternatively, it is possible to obtain the structural details for adduct II and site of substrate attachment by X-ray crystallography. It would be appropriate to study the anti-isonicotinoyl reactivity in western blotting when MP-11 is used with isoniazid. Since Isoniazid has similar structure and reactivity as of benzoic acid hydrazides, the potential of INH in limiting MPO and thereby causing neutrophil toxicity should be looked.

4.4 References

1 Klebanoff, S. J. Myeloperoxidase-halide-hydrogen peroxide antibacterial system. *Journal of bacteriology* **95**, 2131-2138 (1968).

2 Hawkins, C. & Davies, M. Reaction of HOCl with amino acids and peptides: EPR evidence for rapid rearrangement and fragmentation reactions of nitrogen-centred radicals. *Journal of the Chemical Society, Perkin Transactions 2*, 1937-1946 (1998).

3 Kettle, A. J. & Winterbourn, C. C. Mechanism of inhibition of myeloperoxidase by anti-inflammatory drugs. *Biochemical Pharmacology* **41**, 1485-1492 (1991).

4 Kettle, A. J., Gedye, C. A., Hampton, M. B. & Winterbourn, C. C. Inhibition of myeloperoxidase by benzoic acid hydrazides. *Biochemical Journal* **308,** 559-563 (1995).

5 Aitken, S. M., Ouellet, M., Percival, M. D. & English, A. M. Mechanism of horseradish peroxidase inactivation by benzhydrazide: a critical evaluation of arylhydrazides as peroxidase inhibitors. *Biochemical Journal* **375**, 613-621 (2003).

6 Guallar, V. & Wallrapp, F. H. QM/MM methods: looking inside heme proteins biochemistry. *Biophysical Chemistry* **149**, 1-11 (2010).

7 Obinger, C. Heme peroxidase biochemistry - Facts and perspectives. *Archives of Biochemistry and Biophysics* **500**, 1-2 (2010).

8 Badyal, S. K. *et al.* Iron oxidation state modulates active site structure in a heme peroxidase. *Biochemistry* **47**, 4403-4409 (2008).

9 Hiraga, S., Sasaki, K., Ito, H., Ohashi, Y. & Matsui, H. A Large Family of Class III Plant Peroxidases. *Plant and Cell Physiology* **42**, 462-468 (2001).

10 O'Brien, P. J. Peroxidases. *Chemico-Biological Interactions* **129**, 113-139 (2000).

11 Vellosa, J. C. R. Salacia campestris root bark extract: peroxidase inhibition, antioxidant and antiradical profile. *Brazilian Journal of Pharmaceutical Sciences* **45**, 99-107 (2009).

12 Tafazoli, S. & O'Brien, P. J. Peroxidases: a role in the metabolism and side effects of drugs. *Drug Discovery Today* **10**, 617-625 (2005).

13 Ross, D. & Moldeus, P. Generation of reactive species and fate of thiols during peroxidase-catalyzed metabolic activation of aromatic amines and phenols. *Environmental Health Perspectives* **64**, 253-257 (1985).

14 Kappus, H. & Sies, H. Toxic drug effects associated with oxygen metabolism: Redox cycling and lipid peroxidation. *Cellular and Molecular Life Sciences* **37**, 1233-1241 (1981).

15 O'Brien, P. J. Radical formation during the peroxidase catalyzed metabolism of carcinogens and xenobiotics: The reactivity of these radicals with GSH, DNA, and unsaturated lipid. *Free Radical Biology and Medicine* **4**, 169-183 (1988).

16 Klebanoff, S. J. Myeloperoxidase: friend and foe. *Journal of Leukocyte Biology* **77**, 598-625 (2005).

17 Davies, M. J. Myeloperoxidase-derived oxidation: mechanisms of biological damage and its prevention. *Journal of Clinical Biochemistry and Nutrition* **48**, 8-19 (2011).

18 Borregaard, N. & Cowland, J. B. Granules of the Human Neutrophilic Polymorphonuclear Leukocyte. *Blood* **89**, 3503-3521 (1997).

19 Fiedler, T. J., Davey, C. A. & Fenna, R. E. X-ray Crystal Structure and Characterization of Halide-binding Sites of Human Myeloperoxidase at 1.8 Å Resolution. *Journal of Biological Chemistry* **275**, 11964-11971 (2000).

20 Fenna, R., Zeng, J. & Davey, C. Structure of the Green Heme in Myeloperoxidase. *Archives of Biochemistry and Biophysics* **316**, 653-656 (1995).

21 Meotti, F. C. *et al.* Urate as a Physiological Substrate for Myeloperoxidase. *Journal of Biological Chemistry* **286**, 12901-12911 (2011).

22 Halliwell, B. & Gutteridge, J. M. C. *Free Radicals in Biology and Medicine*. 4th edn, (Oxford University Press, 2007).

23 Li, Y. & Trush, M. A. Diphenyleneiodonium, an NAD(P)H Oxidase Inhibitor, also Potently Inhibits Mitochondrial Reactive Oxygen Species Production. *Biochemical and Biophysical Research Communications* **253**, 295-299 (1998).

24 Shacter, E., Lopez, R. L. & Pati, S. Inhibition of the myeloperoxidase-H2O2-Cl- system of neutrophils by indomethacin and other non-steroidal anti-inflammatory drugs. *Biochemical Pharmacology* **41**, 975-984 (1991).

25 Segelmark, M., Persson, B., Hellmark, T. & Wieslander, J. Binding and inhibition of myeloperoxidase (MPO): a major function of ceruloplasmin? *Clinical and Experimental Immunology* **108**, 167-174 (1997).

26 Koelsch, M., Mallak, R., Graham, G. G., Kajer, T., Milligan, M. K., Nguyen, L. Q., Newsham, D. W., Keh, J. S., Kettle, A. J., Scott, K. F., Ziegler, J. B., Pattison, D. I., Fu, S., Hawkins, C. L., Rees, M. D. & Davies, M. J. Acetaminophen (paracetamol) inhibits myeloperoxidase-catalyzed oxidant production and biological damage at therapeutically achievable concentrations. *Biochemical Pharmacology* **79**, 1156-1164 (2010).

27 Galijasevic, S., Abdulhamid, I. & Abu-Soud, H. M. Potential role of tryptophan and chloride in the inhibition of human myeloperoxidase. *Free Radical Biology & Medicine* **44**, 1570-1577 (2008).

28 Siraki, A. G., Bonini, M. G., Jiang, J., Ehrenshaft, M. & Mason, R. P. Aminoglutethimide-induced protein free radical formation on myeloperoxidase: a potential mechanism of agranulocytosis. *Chemical Research in Toxicology* **20**, 1038-1045 (2007).

29 Siraki, A. G., Deterding, L. J., Bonini, M. G., Jiang, J., Ehrenshaft, M., Tomer, K. B. & Mason, R. Procainamide, but not N-acetylprocainamide, induces protein free radical formation on myeloperoxidase: a potential

mechanism of agranulocytosis. *Chemical Research in Toxicology* **21**, 1143-1153 (2008).

30 Kettle, A. J. & Winterbourn, C. C. Oxidation of hydroquinone by myeloperoxidase. Mechanism of stimulation by benzoquinone. *Journal of Biological Chemistry* **267**, 8319-8324 (1992).

31 Kettle, A. J., Robertson, I. G., Palmer, B. D., Anderson, R. F., Patel, K. B. & Winterbourn, C. C. Oxidative metabolism of amsacrine by the neutrophil enzyme myeloperoxidase. *Biochemical Pharmacology* **44**, 1731-1738 (1992).

32 van Zyl, J. M., Basson, K., Uebel, R. A. & van der Walt, B. J. Isoniazid-mediated irreversible inhibition of the myeloperoxidase antimicrobial system of the human neutrophil and the effect of thyronines. *Biochemical Pharmacology* **38**, 2363-2373, doi:10.1016/0006-2952(89)90477-2 (1989).

33 Ranguelova, K., Suarez, J., Magliozzo, R. S. & Mason, R. P. Spin Trapping Investigation of Peroxide- and Isoniazid-Induced Radicals in Mycobacterium tuberculosis Catalase-Peroxidase. *Biochemistry* **47**, 11377-11385 (2008).

34 Cade, C. E., Dlouhy, A. C., Medzihradszky, K. F., Salas-Castillo, S. P. & Ghiladi, R. A. Isoniazid-resistance conferring mutations in Mycobacterium tuberculosis KatG: catalase, peroxidase, and INH-NADH adduct formation activities. *Protein science : a publication of the Protein Society* **19**, 458-474 (2010).

35 Hofstra, A. H., Li-Muller, S. M. & Uetrecht, J. P. Metabolism of isoniazid by activated leukocytes. Possible role in drug-induced lupus. *Drug Metabolism and Disposition: The Biological Fate of Chemicals* **20**, 205-210 (1992).

36 Ator, M. A. & Ortiz de Montellano, P. R. Protein control of prosthetic heme reactivity. Reaction of substrates with the heme edge of horseradish peroxidase. *Journal of Biological Chemistry* **262**, 1542-1551 (1987).

37 Ator, M. A., David, S. K. & Ortiz de Montellano, P. R. Structure and catalytic mechanism of horseradish peroxidase. Regiospecific meso alkylation of the prosthetic heme group by alkylhydrazines. *Journal of Biological Chemistry* **262**, 14954-14960 (1987).

38 Pierattelli, R., Banci, L., Eady, N. A. J., Bodiguel, J., Jones, J. N., Moody, P. C. E., Raven, E. L., Jamart-Grégoire, B. & Brown, K. A. Enzyme-catalyzed Mechanism of Isoniazid Activation in Class I and Class III Peroxidases. *Journal of Biological Chemistry* **279**, 39000-39009 (2004).

39 Sinha, B. K. Enzymatic activation of hydrazine derivatives. A spin-trapping study. *Journal of Biological Chemistry* **258**, 796-801 (1983).

40 Kettle, A. J., Gedye, C. A. & Winterbourn, C. C. Mechanism of inactivation of myeloperoxidase by 4-aminobenzoic acid hydrazide. *Biochemical Journal* **321**, 503-508 (1997).

41 Nazari, K., Mahmoudi, A., Khosraneh, M., Haghighian, Z. & Moosavi-Movahedi, A. A. Kinetic analysis for suicide-substrate inactivation of microperoxidase-11: A modified model for bisubstrate enzymes in the

presence of reversible inhibitors. *Journal of Molecular Catalysis B: Enzymatic* **56**, 61-69 (2009).

42 Dickerson, R. E. The structures of cytochrome c and the rates of molecular evolution. *Journal of Molecular Evolution* **1**, 26-45 (1971).

43 Marques, H. M. Insights into porphyrin chemistry provided by the microperoxidases, the haempeptides derived from cytochrome c. *Dalton Transactions* 4371-4385 (2007).

44 Osman, A. M., Koerts, J., Boersma, M. G., Boeren, S., Veeger, C., and Rietjens, I. M. (1996) European journal of biochemistry / FEBS 240, 232- Microperoxidase/H2O2-catalyzed aromatic hydroxylation proceeds by a cytochrome-P-450-type oxygen-transfer reaction mechanism. *European Journal of Biochemistry / FEBS* **240**, 232-238 (1996).

45 Khosraneh, M., Mahmoudi, A., Rahimi, H., Nazari, K. & Moosavi-Movahedi, A. A. Suicide-peroxide inactivation of microperoxidase-11: a kinetic study. *Journal of Enzyme Inhibition Medicianl Chemistry* **22**, 677-684 (2007).

46 Spector, A., Ma, W., Wang, R. R. & Kleiman, N. J. Microperoxidases catalytically degrade reactive oxygen species and may be anti-cataract agents. *Experimental Eye Research* **65**, 457-470 (1997).

47 Spector, A., Zhou, W., Ma, W., Chignell, C. F. & Reszka, K. J. Investigation of the mechanism of action of microperoxidase-11, (MP11), a potential anti-cataract agent, with hydrogen peroxide and ascorbate. *Experimental Eye Research* **71**, 183-194 (2000).

48 Fischer, V., West, P. R., Harman, L. S. & Mason, R. P. Free-radical metabolites of acetaminophen and a dimethylated derivative. *Environmental Health Perspectives* **64**, 127-137 (1985).

49 Janzen, E. G., Stronks, H. J., Dubose, C. M., Poyer, J. L. & McCay, P. B. Chemistry and biology of spin-trapping radicals associated with halocarbon metabolism in vitro and in vivo. *Environmental Health Perspectives* **64**, 151-170 (1985).

50 Mason, R. P. Using anti-5,5-dimethyl-1-pyrroline N-oxide (anti-DMPO) to detect protein radicals in time and space with immuno-spin trapping. *Free Radical Biology and Medicine* **36**, 1214-1223(2004).

51 Williams, F. Electron Paramagnetic Resonance: Elementary Theory and Practical Applications, Second Edition (John A. Weil and James R. Bolton). *Journal of Chemical Education* **86**, 33 (2009).

52 Buettner, G. R. & Mason, R. P. Spin-trapping methods for detecting superoxide and hydroxyl free radicals in vitro and in vivo. *Methods in Enzymology* **186**, 127-133 (1990).

53 Amos, R. I. J., Gourlay, B. S., Schiesser, C. H., Smith, J. A. & Yates, B. F. A mechanistic study on the oxidation of hydrazides: application to the tuberculosis drug isoniazid. *Chemical Communications*, 1695-1697 (2008).

54 Gomez-Mejiba, S. E. Zhai, Z., Akram, H., Deterding, L. J., Hensley, K., Smith, N., Towner, R. A., Tomer, K. B., Mason, R. P., & Ramirez, D. C. Immuno-spin trapping of protein and DNA radicals: "tagging" free

radicals to locate and understand the redox process. *Free Radical Biology & Medicine* **46**, 853-865 (2009).

55 Nakamura, S., Mashino, T. & Hirobe, M. 18O incorporation from H2 18O2 in the oxidation of N-methylcarbazole and sulfides catalyzed by microperoxidase-11. *Tetrahedron Letters* **33**, 5409-5412 (1992).

56 Nelson, D. P. & Kiesow, L. A. Enthalpy of decomposition of hydrogen peroxide by catalase at 25Â° C (with molar extinction coefficients of H2O2 solutions in the UV). *Analytical Biochemistry* **49**, 474-478 (1972).

57 Jiang, T. & Yuan, Z. in *Handbook of Food Enzymology* (CRC Press, 2002).

58 Baldwin, D. A., Marques, H. M. & Pratt, J. M. Hemes and Hemoproteins. 5: Kinetics of the Peroxidatic Activity of Microperoxidase-8: Model for the Peroxidase Enzymes. *Journal of Inorganic Biochemistry* **30**, 203-217 (1987).

59 Zhang, N., Doucette, A. & Li, L. Two-Layer Sample Preparation Method for MALDI Mass Spectrometric Analysis of Protein and Peptide Samples Containing Sodium Dodecyl Sulfate. *Analytical Chemistry* **73**, 2968-2975 (2001).

60 Sobieszek, A. & Jertschin, P. Urea-glycerol-acrylamide gel electrophoresis of acidic low molecular weight muscle proteins: Rapid determination of myosin light chain phosphorylation in myosin, actomyosin and whole muscle samples. *Electrophoresis* **7**, 417-425 (1986).

61 Siraki, A. G., Jiang, J. & Mason, R. P. Investigating the Mechanisms of Aromatic Amine-Induced Protein Free Radical Formation by Quantitative Structure−Activity Relationships: Implications for Drug-Induced Agranulocytosis. *Chemical Research in Toxicology* **23**, 880-887 (2010).

62 Burner, U., Obinger, C., Paumann, M., Furtmuller, P. G. & Kettle, A. J. Transient and steady-state kinetics of the oxidation of substituted benzoic acid hydrazides by myeloperoxidase. *Journal of Biological Chemistry* **274**, 9494-9502 (1999).

63 Winder, F. G. & Denneny, J. M. Metal-catalysed auto-oxidation of isoniazid. *Biochemical Journal* **73**, 500-507 (1959).

64 Choe, Y. S. & Ortiz de Montellano, P. R. Differential additions to the myoglobin prosthetic heme group. Oxidative gamma-meso substitution by alkylhydrazines. *Journal of Biological Chemistry* **266**, 8523-8530 (1991).

65 Gamberini, M., Cidade, M. R., Valotta, L. A., Armelin, M. C. & Leite, L. C. Contribution of hydrazines-derived alkyl radicals to cytotoxicity and transformation induced in normal c-myc-overexpressing mouse fibroblasts. *Carcinogenesis* **19**, 147-155 (1998).

66 Misra, H. P. & Fridovich, I. The oxidation of phenylhydrazine: superoxide and mechanism. *Biochemistry* **15**, 681-687 (1976).

67 Sinha, B. K. & Motten, A. G. Oxidative metabolism of hydralazine. Evidence for nitrogen centered radicals formation. *Biochemical and Biophysical Research Communications* **105**, 1044-1051 (1982).

68 Yamashoji, S. Determination of viable mammalian cells by luminol chemiluminescence using microperoxidase. *Analytical Biochemistry* **386**, 119-120 (2009).

69 Niederländer, H. A. G., Gooijer, C. & Velthorst, N. H. Chemiluminescence detection in liquid chromatography based on photo-oxygenation involving reactive oxygen intermediates. *Analytica Chimica Acta* **285**, 143-159 (1994).

70. Zhang H., Yang S., Xu H. & Kirkwood P. Peptide-based peroxidase inhibitors and methods of using same. *Patent Co-operation Treaty*, **WO2011/044096 A1** (2011).